Facies, stratigraphy, and evolution of a middle Ediacaran carbonate ramp: Khufai Formation, Sultanate of Oman

Magdalena Osburn, John Grotzinger, and Kristin Bergmann

ABSTRACT

The Khufai Formation is the oldest carbonate platform of the Cryogenian to lowermost Cambrian Huqf Supergroup. A stratigraphic characterization of this unit includes detailed facies descriptions, a sequence-stratigraphic interpretation, and evaluation of lateral heterogeneity and overall ramp evolution. The Khufai Formation comprises one and one-half depositional sequences with a maximum flooding interval near the base of the formation and a sequence boundary within the upper peritidal facies. Most of the deposition occurred during highstand progradation of a carbonate ramp. Facies tracts include outer-ramp and midramp mudstones and wackestones, ramp-crest grainstone shoal deposits, and extensive inner-ramp, microbially dominated peritidal deposits. Outcrops in the Oman Mountains are deep-water deposits, including turbiditic grainstone and wackestone interbedded with siliciclastic-rich siltstone and crinkly laminite. Facies patterns and parasequence composition are variable both laterally across the outcrop area and vertically through time because of a combination of ramp morphology, siliciclastic supply, and possible syndepositional faulting. The lithostratigraphic boundary between the Khufai Formation and the overlying Shuram Formation is gradational and represents significant flooding of the carbonate platform. The stratigraphic characterization presented here along with the identification of key facies and diagenetic features will help further future exploration and production of hydrocarbons from the Khufai Formation.

Manuscript received January 30, 2013; provisional acceptance November 27, 2012; revised manuscript received January 31, 2013; final acceptance July 29, 2013.
DOI: 10.1306/07291312140

AUTHORS

MAGDALENA OSBURN ~ *California Institute of Technology, 1200 E. California Boulevard, Pasadena, California; maggie@earth.northwestern.edu*

Magdalena Osburn is a geobiologist who uses sedimentology and organic geochemistry to understand the history of life on Earth and microbial influences on biogeochemical processes. She has a B.A. degree in earth and planetary sciences from Washington University in St. Louis and a Ph.D. in geobiology from the California Institute of Technology.

JOHN GROTZINGER ~ *California Institute of Technology, 1200 E. California Boulevard, Pasadena, California; grotz@caltech.edu*

John Grotzinger is a geologist interested in the evolution of surficial environments on Earth and Mars. Field mapping studies are the starting point for more topical laboratory-based studies involving geochemical, geological, and geochronological techniques.

KRISTIN BERGMANN ~ *California Institute of Technology, 1200 E. California Boulevard, Pasadena, California; bergmann@caltech.edu*

Kristin Bergmann received degrees in geology from Carleton College (B.A. degree) and the California Institute of Technology (M.Sc. degree) where she is currently a Ph.D. candidate. She is studying the carbonate sedimentology, stratigraphy, and geochemistry of units within the Huqf Supergroup and is applying carbonate clumped isotope thermometry to problems of carbonate diagenesis and paleoclimate.

ACKNOWLEDGEMENTS

We thank William Wilks, Gordon Forbes, Gideon Lopes-Cardozo, Joachim Amthor, and other Petroleum Development Oman personnel for helpful discussions; Salim Al Maskery for field support and logistics; the participants of the 2009 Agouron Advanced Field Course for initial stratigraphic observation; the Ministry of Oil and Gas, Sultanate of Oman, for permission to

conduct and publish this research; and Michael Pope, Erwin Adams, and Stephan Schroder for helpful and constructive reviews.
The AAPG Editor thanks the following reviewers for their work on this paper: Erwin W. Adams, Michael Pope, and Stefan Schroeder.

EDITOR'S NOTE

Color versions of Figures 6–13 can be seen in the online version of his paper.

INTRODUCTION

Neoproterozoic strata of Oman provide an exceptionally complete and well-preserved sedimentary record of a highly variable period in Earth history. Recorded in these sediments are two of the proposed Snowball Earth glaciations, the largest carbon isotopic excursion in Earth history, the origination of Ediacaran calcified metazoans, and the Precambrian–Cambrian boundary (Burns and Matter, 1993; Wood et al., 2002; Allen, 2007; Bowring et al., 2007). In addition, the Huqf Supergroup hosts the oldest commercially viable hydrocarbon system with producing reservoirs in uppermost Ediacaran to lowermost Cambrian rocks (Al-Siyabi, 2005).

Regional stratigraphic surveys of the Huqf Supergroup provide a basic understanding of the depositional setting, and chemostratigraphic studies document concurrent changes in marine chemistry and enhance regional stratigraphic correlation (Wright et al., 1990; Burns and Matter, 1993; McCarron, 1999; Halverson, 2005; Fike et al., 2006; Le Guerroue et al., 2006a; Fike and Grotzinger, 2008). Considerable attention was devoted to understanding the older siliciclastic Masirah Bay Formation shelf sequence (Allen and Leather, 2006), the overlying Shuram Formation (Le Guerroue et al., 2006a), and the younger Buah Formation carbonate ramp (Cozzi and Grotzinger, 2004; Cozzi et al., 2004). Conversely, relatively little is known about Khufai Formation development, beyond its inclusion in regional surveys (Gorin et al., 1982; Wright et al., 1990; McCarron, 1999).

A firm understanding of sedimentological and stratigraphic context is necessary for evaluation of both geochemical measurements and the potential for hydrocarbon exploration. We have undertaken this study to better understand the processes, environments, and time scale of Khufai Formation deposition. This article presents an analysis of the facies distributions from both platform and distal sections along with a detailed sequence-stratigraphic interpretation of the Khufai Formation. We evaluate the stratigraphic position and extent of depositional hiatuses in the upper Khufai Formation to better interpret chemostratigraphic records. The presentation of key facies and facies relationships in stratigraphic context will provide a valuable framework for future hydrocarbon exploration and development.

Geological Setting

The Huqf Supergroup is a sequence of Cryogenian to Lower Cambrian sedimentary rocks, deposited on Archean to Neoproterozoic crystalline basement (Allen, 2007; Bowring et al., 2007). Huqf strata outcrop in four main areas including the

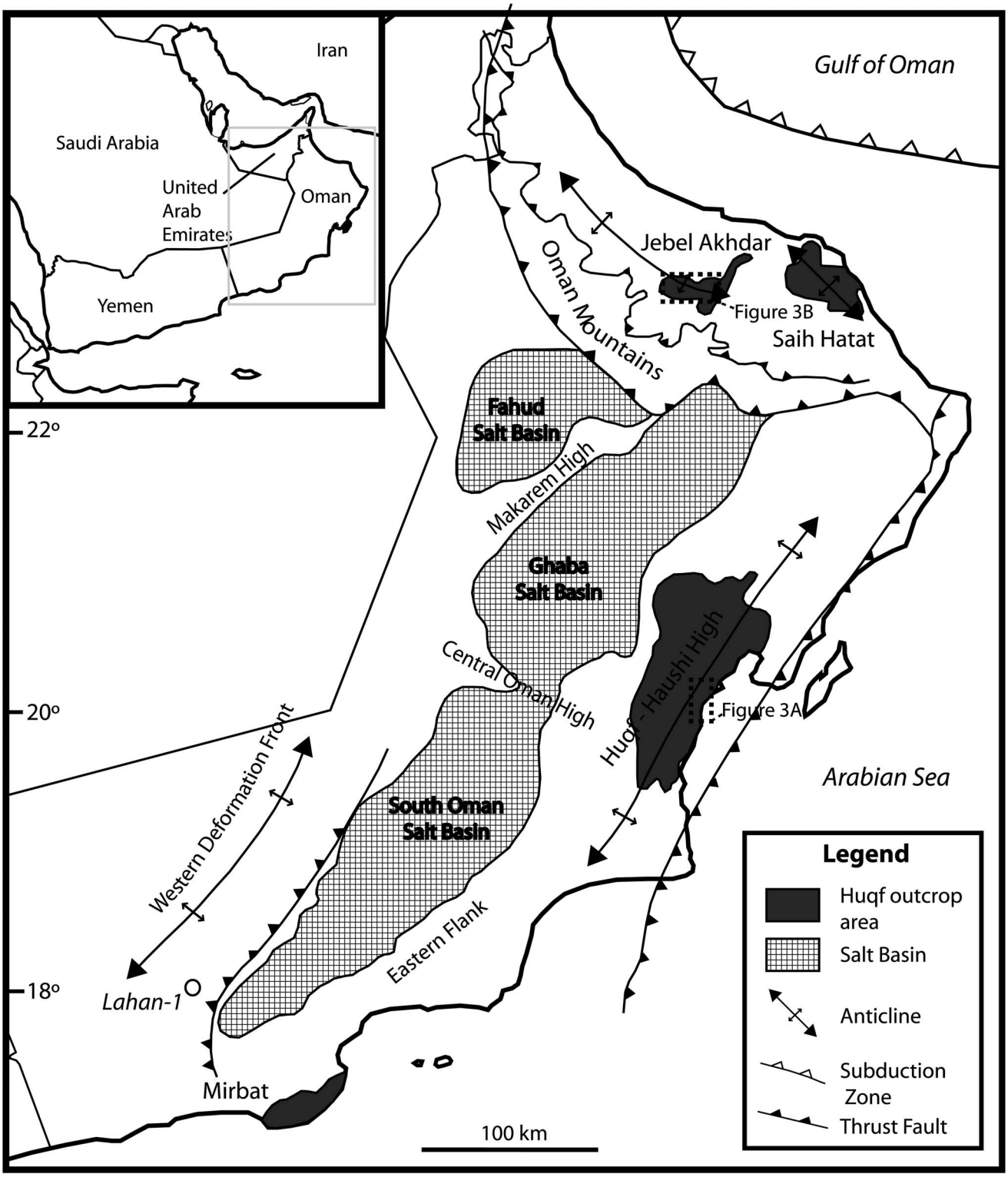

Figure 1. Regional map of Oman illustrating the outcrop localities for the Huqf Supergroup, regional tectonic features, and salt basins. Modified after Bowring et al. (2007).

Huqf-Haushi uplift and Mirbat areas of central and southern Oman and near Jebel Akhdar and Saih Hatat in the Oman Mountains (Figure 1). The Huqf Supergroup comprises, in ascending order, the Abu Mahara, Nafun, and Ara Groups representing glaciomarine sediments, marine siliciclastics and

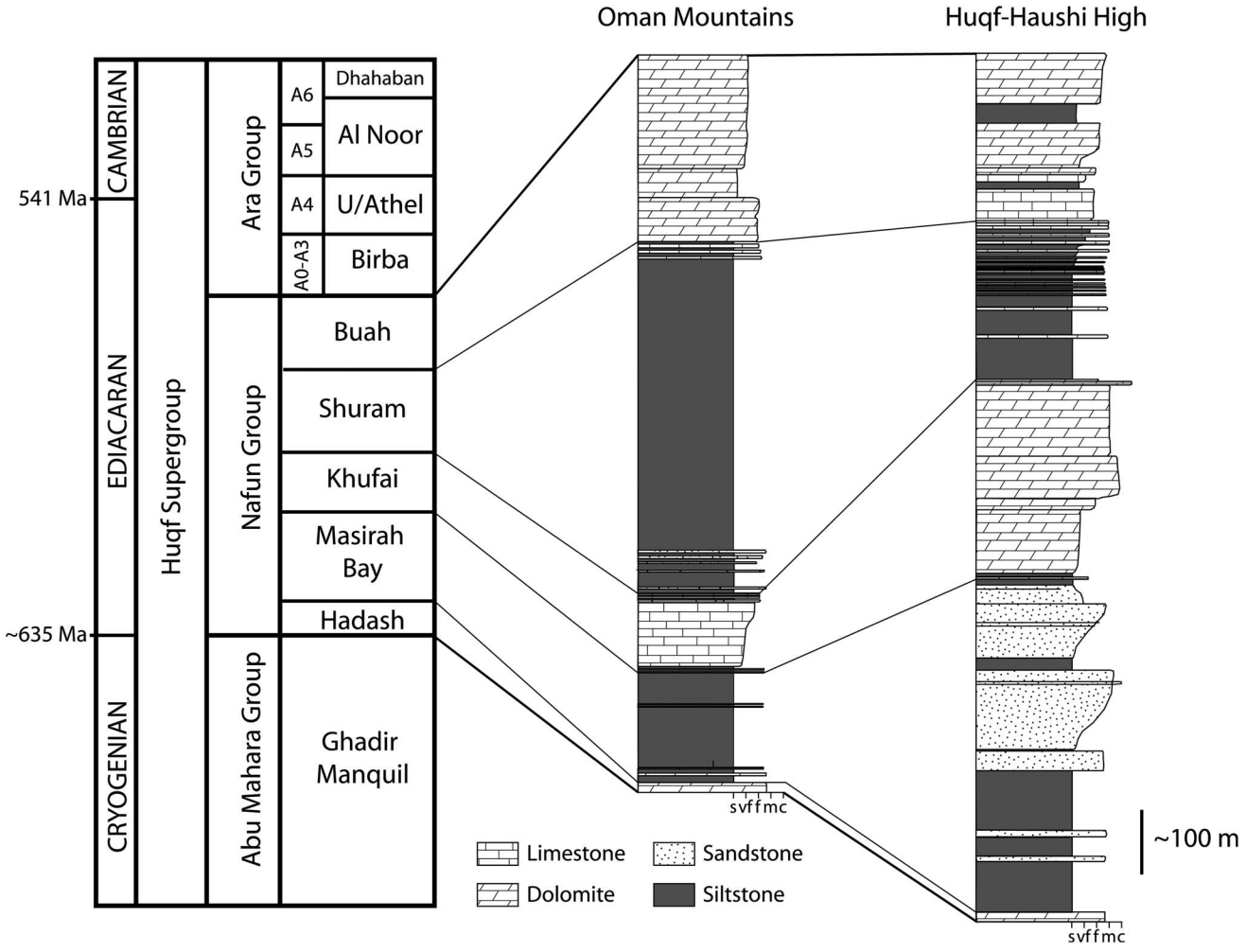

Figure 2. Stratigraphic nomenclature for the Huqf Supergroup. Basic lithostratigraphic logs of the Nafun Group in the Huqf-Haushi high and Oman Mountain areas. Modified after Forbes et al. (2010), Bowring et al. (2007), McCarron (1999), and Allen and Leather (2006).

carbonates, and carbonates cyclically interstratified with sulfate and halite evaporites, respectively. The Nafun Group was further subdivided (Figure 2) into the successive Hadash, Masirah Bay, Khufai, Shuram, and Buah Formations (Gorin et al., 1982; Wright et al., 1990; Forbes et al., 2010). The Hadash Formation is a thin dolostone capping the Ghadir Manquil (Marinoan) glacial deposits, but is included in the Nafun Group. The overlying four units comprise two large siliciclastic-to-carbonate cycles; where the Masirah Bay and Shuram Formations contain primarily siltstone and sandstone with minor carbonate, and the Khufai and Buah Formations contain primarily carbonate facies with subordinate siliciclastic components (Forbes et al., 2010). The Nafun Group is well exposed on the Huqf-Haushi uplift (Huqf area) and in the wadis of Jebel Akhdar.

Age Control and Tectonic Setting

The absolute ages of the Abu Mahara and Ara Groups are relatively well constrained by U-Pb dating, but few chronostratigraphic constraints exist in the intervening Nafun Group. The Abu Mahara Group is deposited on approximately 824 m.y.-old granodioritic basement (Bowring et al., 2007). A tuffaceous sandstone within the Ghubrah Member of the lower Abu Mahara Group was deposited at approximately 713 Ma (Bowring et al., 2007), revising upward a previous date of 723 + 16/-10 Ma

(Brasier et al., 2000). A population of zircons from Petroleum Development Oman (PDO), Lahan-1, well gives a maximum age constraint of 645 Ma for the youngest glacial deposits. Furthermore, global correlation with glacial events suggest a correlative date of the Hadash cap carbonate of about 635 Ma (Bowring et al., 2007). The Ara Group has several ash beds ranging in age from 546 ± 0.21 Ma in the A0 interval, to 541.00 ± 0.13 Ma in the A4C (Bowring et al., 2007). Sedimentation rates from well-dated sections of the upper Buah Formation and Ara Group were extrapolated to give an approximate age of the basal Shuram Formation of 554 to 562 Ma. This analysis assumed a significant depositional hiatus at the Khufai-Shuram boundary and, thus, does not constrain the age of the Khufai Formation.

The tectonic setting of the Nafun Group is also not well constrained. A suture zone in Yemen and arc-related volcanic basement of the Huqf suggests accretion of the Oman terrain onto the Arabian–Nubian plate prior to the deposition of Nafun strata. The Abu Mahara sediments and volcanics accumulated in extensional basins, whereas subsequent sedimentary deposition was regionally extensive and suggestive of relative tectonic quiescence (Allen, 2007). Accommodation for the Nafun Group was created primarily through thermal contraction of the crust in a passive margin sequence (Allen, 2007). Others have argued that this mechanism is insufficient to accommodate the whole of the Nafun Group and suggest dynamic lithospheric depression related to subduction (Grotzinger and Amthor, 2002; Grotzinger et al., 2002). Significant transtensional tectonic and volcanic activity resumed during Ara deposition, creating the South Oman, Ghaba, and Fahud evaporite basins (Grotzinger and Amthor, 2002; Allen, 2007; Bowring et al., 2007).

The Nafun Group

Previous work has focused on the deposition and sedimentary features of the Nafun Group as a whole (Gorin et al., 1982; McCarron, 1999; Forbes et al., 2010), with additional studies focusing on aspects of the Masirah Bay (Allen and Leather, 2006), Shuram (Le Guerroue et al., 2006a, b), and Buah (Cozzi and Grotzinger, 2004) Formations, and Ara Group (Mattes and Conway Morris, 1990). The Khufai Formation was initially interpreted as a uniformly shallow platform carbonate with abundant evaporitic collapse features (Gorin et al., 1982). Subsequent interpretations have favored a prograding ramp model with the basal strata representing subwave base deposition (Wright et al., 1990; McCarron, 1999). The lower contact between the Masirah Bay Formation and the Khufai Formation is gradational, displaying interfingering of siltstones and carbonates over several meters of the contact (Allen and Leather, 2006).

Little agreement exists on the nature of the lithostratigraphic contact between the Khufai and Shuram Formations. Citing unpublished seismic data from Petroleum Development Oman and a potential localized karstic surface, some favor a significant depositional hiatus and major sequence boundary (McCarron, 1999; Bowring et al., 2007; Forbes et al., 2010). Others have noted minor hardground features in an oolite marking the uppermost Khufai Formation, but do not assign significant time to the boundary (Wright et al., 1990).

The Khufai Formation represents a key interval in Earth history, capturing the onset of a global negative excursion in the isotopic composition of carbonate carbon (Grotzinger et al., 2011), but has lacked complete characterization regarding its facies, stratigraphy, and ramp evolution. This excursion was first observed in Oman (Burns and Matter, 1993) and is initially recorded by the upper Khufai Formation, reaching a minimum in the overlying Shuram Formation, and increasing to the baseline well into the Buah Formation (Fike et al., 2006; Le Guerroue et al., 2006c). Multiple explanations for this excursion have been proposed, including some that have significant implications for the oxidation state of the global ocean and the evolution of the Ediacaran fauna (Grotzinger et al., 2011).

Distribution of Khufai Formation

The Khufai Formation is best exposed in the Huqf area and in Jebel Akhdar. Continuous sections of the Khufai Formation exist in the Huqf area outcrop within three large anticlinal domes: the Mukhaibah, Khufai, and Buah domes (Figure 3A). These

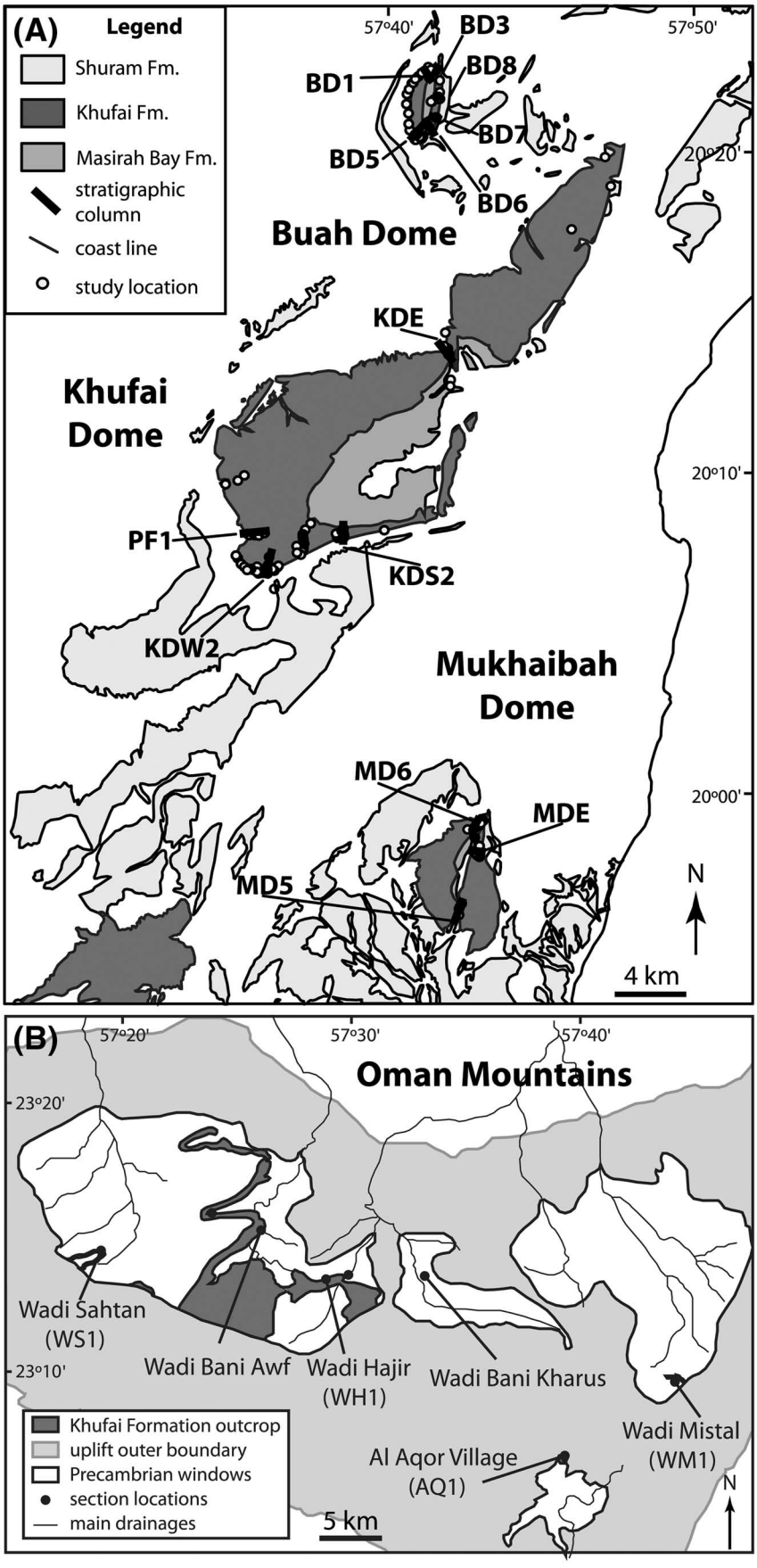

Figure 3. Geological map showing study locations and stratigraphic sections. (A) Geological map of the Huqf area showing the distribution of the Masirah Bay, Khufai, and Shuram Formations and domes are discussed in the text. (B) Sketch map of the Oman Mountains defined by the outer boundary of sedimentary uplift (gray). Erosional windows into the Precambrian are shown in white, and the Khufai Formation outcrop is in dark gray. Names and paths of major wadis are shown for reference.

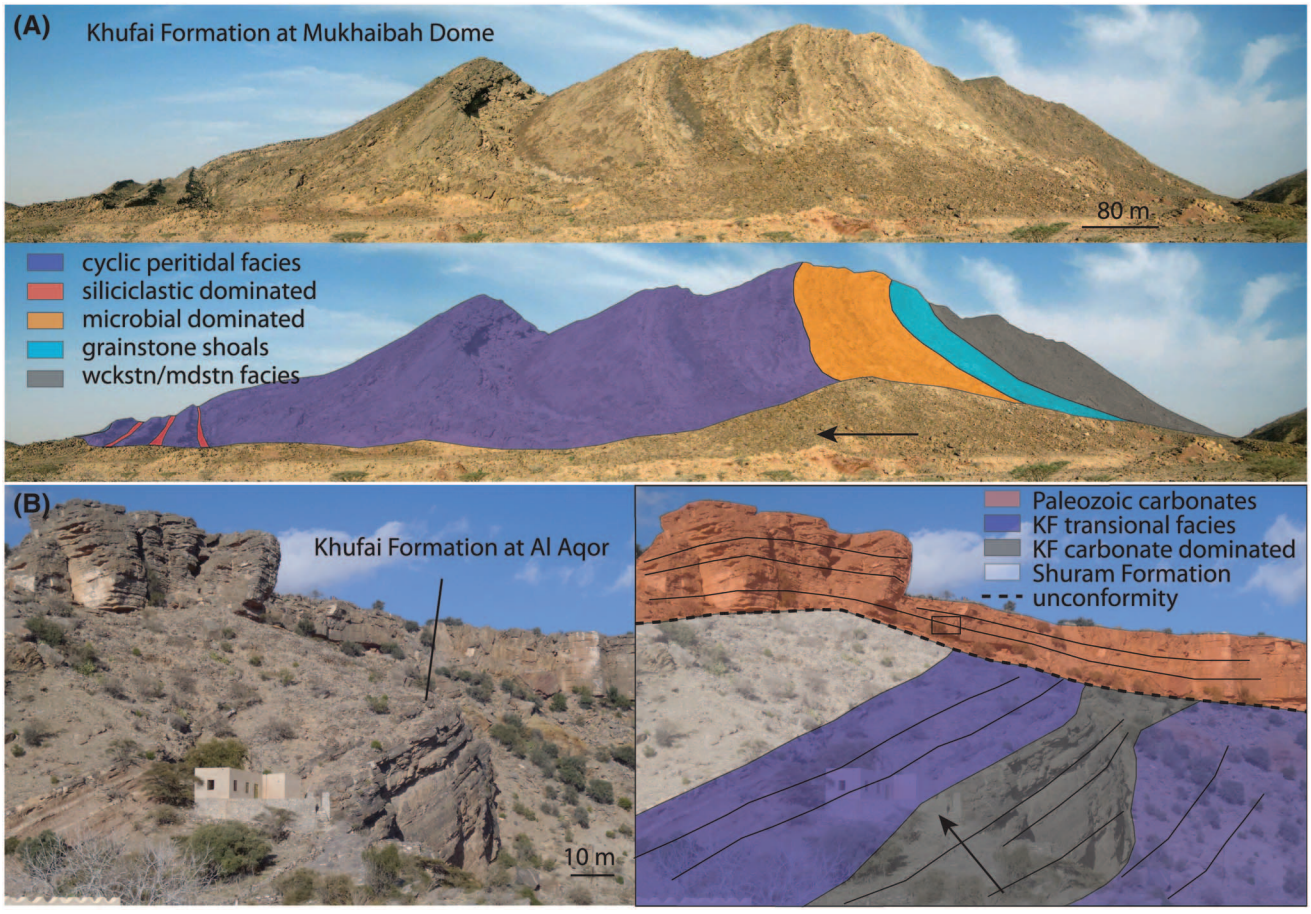

Figure 4. Interpreted outcrop photos from (A) Mukhaibah dome and (B) Al Aqor village in the Oman Mountains illustrating major facies groups.

locations feature generally good textural preservation and minimal structural deformation beyond the simple, open folds that define the domes. Primary carbonate sediments were pervasively dolomitized, which obscures fine depositional detail in strongly affected intervals. This contrasts with exposures in the core of the Jebel Akhdar uplift in the Oman Mountains (Figure 3B), where the Khufai Formation shows extensive ductile folding with associated penetrative cleavage, severe neomorphic recrystallization, and extensive faulting.

The Khufai Formation in the Huqf area is approximately 300 to 320 m (1000 to 1050 ft) thick and forms a modern topographic high (Figure 4A). Both upper and lower contacts appear to be gradational, although the upper contact is rarely preserved. A regionally extensive, Tertiary-aged erosional event truncated the Khufai Formation preserved in the anticlines and left erosional peneplanation surfaces mantled in thick siliceous breccias. Differential erosion of the Khufai Formation compared to the Masirah Bay and Shuram Formations commonly obscures the contacts and creates a steep gradient between the peneplanation surface and the valley floor 100 m (320 ft) below (Figure 4A). The Khufai Formation in the Oman Mountains is primarily composed of black, sulfurous limestone with gradational upper and lower contacts (Figure 4B). The lower and upper contacts are preserved within mixed siliciclastic-carbonate transitional members that are consistently approximately 30 m (100 ft) thick. In contrast, the main phase of carbonate deposition shows significant thickness variability, ranging from 20 to 122 m (66 to 400 ft) (Figure 5). Although extensive folding adds error to thickness determinations, the stratigraphic variability appears to mimic primary bed thickness and grain-size variations.

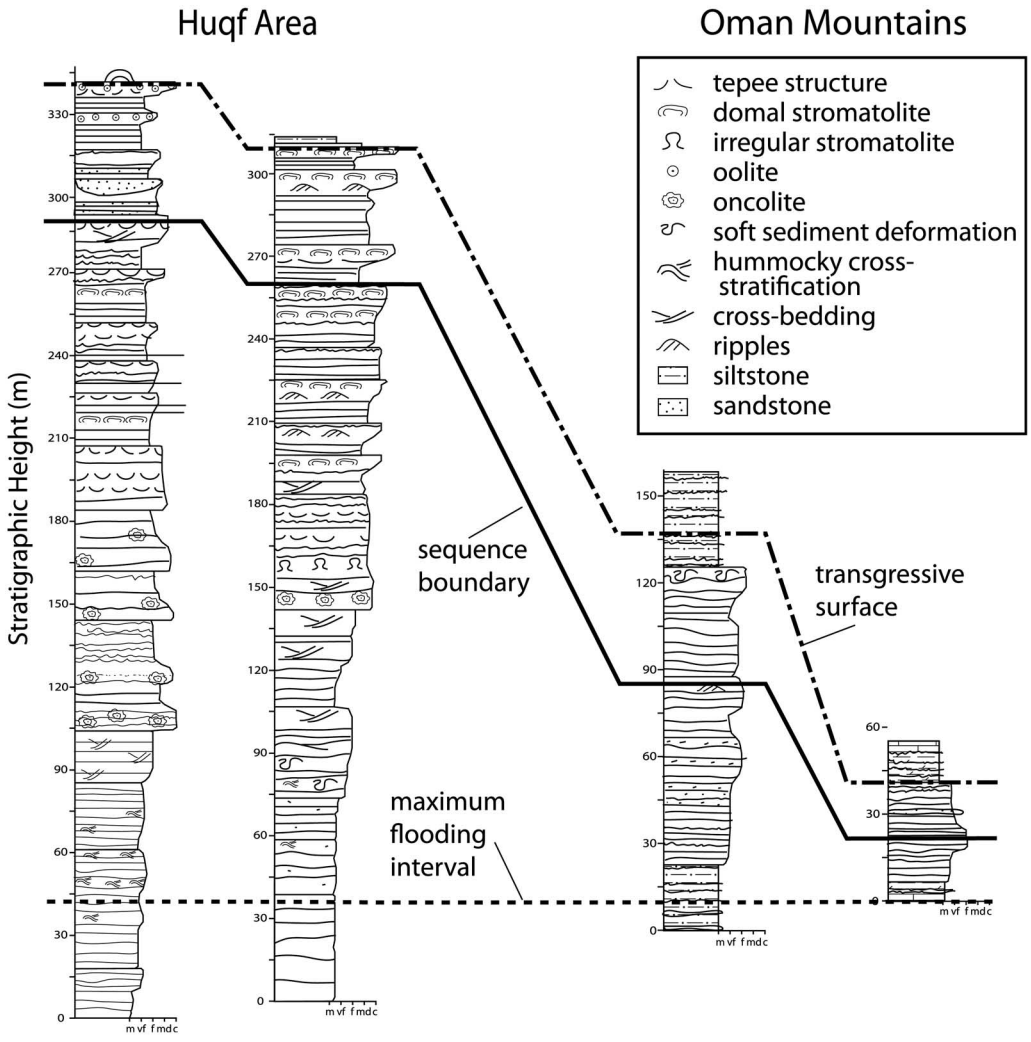

Figure 5. Generalized stratigraphic columns from the Huqf and Oman Mountains illustrating low-resolution facies variability and the position of major stratigraphic surfaces: MFI (dashed line), SB (solid line), TS (dot and dashed line).

METHODS

A total of eight stratigraphic sections covering the full Khufai Formation stratigraphy and seven shorter sections were logged in the Huqf area, covering a modern plan view distance of approximately 85 km (53 mi) (Figure 3A). Five complete sections and one partial section were logged in the Oman Mountains, covering 55 km (34 mi) (Figure 3B). Stratigraphic sections document facies patterns, diagenetic overprints, and parasequence stacking with approximately 10-cm (4-in.) resolution. Samples were collected for slab-scale textural analysis and petrographic analysis.

The stratigraphic architecture of the Khufai Formation was analyzed in hierarchical order beginning with parasequences, followed by parasequence sets, and ramp architecture as a whole. Meter-scale parasequences are easily recognizable in outcrop and combine to form a maximum of four orders of cycles, including parasequence, parasequence set (PS1), compound parasequence set (PS2), and sequence. Parasequences are the smallest observable scale of variability described from observations of accommodation minima and maxima within sets of depositional facies. The sequence is the largest scale of viability observed and corresponds to the formation scale. Ramp geometry was determined from facies and facies stacking patterns within the parasequences.

FACIES AND FACIES TRACTS: HUQF AREA

Depositional facies of the Khufai Formation in the Huqf area and the Oman Mountains differ significantly and are discussed separately. The Huqf area defines a broadly shallowing-upward ramp sequence.

The lower Khufai Formation is characterized by outer-ramp facies with little evidence for storm-wave reworking, whereas the upper Khufai Formation is characterized by peritidal and supratidal deposits. Following the nomenclature of Burchette and Wright (1992), we define outer-, middle-, and inner-ramp facies and group them into facies tracts following the model of Tinker (1998). In this usage, facies tracts contain genetically linked facies and facies successions that record a discrete energy, water depth, and sediment supply setting (Tinker, 1998). The most distal facies form the outer- and middle-ramp facies tracts, whereas the inner ramp is more complex and is subdivided by energy and water depth into subtidal, variable-energy subtidal to intertidal, high-energy subtidal to intertidal, and intertidal to supratidal facies tracts. Finally, where the Khufai Formation includes abundant siliciclastic material, it is appropriate to erect a final facies tract: siliciclastic-influenced facies. The composition of these facies tracts and descriptions of individual facies are summarized in Table 1 and detailed in the text below.

Outer-Ramp Facies Tract

The outer-ramp facies tract consists of peloidal intraclast wackestone and packstone, thick-laminated mudstone, rare intraclast breccia, and siliciclastic siltstone facies. These facies intercalate with those of the middle-ramp facies tract to form a 90- to 130-m (295- to 437-ft)-thick, laterally continuous blanket that records the transgressive systems tract (TST) and maximum flooding interval (MFI) of the lower Khufai Formation. A continuous mineralogic gradation from underlying siliciclastic siltstones of the Masirah Bay is recorded by the transitional contact and intercalation of siltstone into overlying carbonate facies for the first ~10 m (~33 ft) of the formation (Figure 6A). The carbonate sediments reflect alternations between fallout of suspended fine carbonate mud and storm-remobilized density currents containing inner-ramp–derived intraclasts.

Peloidal Intraclast Wackestone and Packstone

Peloidal intraclast wackestone or packstone comprises the bulk of the outer-ramp facies tract. Beds are meter scale and wavy, with scoured bases and cream-colored mudstone intraclasts millimeters to centimeters long concentrated at bed bases. The matrix is dark-gray dolomite mudstone or gray, peloidal, very fine grained packstone and was pervasively dolomitized to a very fine interlocking crystalline fabric (Figure 6C). At the Buah dome, the intraclasts can be much larger (centimeter scale) and more abundant than in the Khufai and Mukhaibah domes grading into a matrix-supported pebble conglomerate. This facies records downramp export of sediment by storm-generated currents consistent with a distal setting (Tucker and Wright, 1990; Betzler et al., 1999). In this subwave base setting, density currents produced by storms would be sufficient to transport peloids and intraclasts from the inner-ramp to the outer-ramp environment (Schlager et al., 1994). Remobilization of pelagic mud accumulations creates the observed matrix components. Intraclasts show facies composition and early lithification more characteristic of inner-ramp shallower water facies and were thus likely eroded and incorporated into deeper water deposits (e.g., Fairchild and Herrington, 1989).

Thick-Laminated Mudstone

The thick-laminated mudstone forms meter-scale beds in the lower Khufai Formation outwardly resembling the wackestones described above. Laminae are centimeter scale and discontinuous, forming an irregular fabric that is highlighted by silicification and dedolomitization. No evidence for wave reworking exists. We interpret this facies to record a low-energy depositional environment below storm-wave base (McCarron, 1999). Thin silty to micritic laminae separating thin packages were previously interpreted as benthic microbial colonization (McCarron, 1999); however, it is alternatively suggested here that this fabric represents pelagic fallout and accumulation of suspended organic material or detritus.

Intraclast Breccia

Intraclast breccias are rare and consist of very coarse, matrix-supported breccia with laminated mudstone clasts (1 to 20 cm [0.4 to 8 in.] in length), occurring in 1–5-m (3.3–16.5-ft)-thick laterally discontinuous lenses. The matrix is muddy; however,

Table 1. Facies and Facies Tracts of the Khufai Formation: Huqf Area

Facies	Location*	Description	Interpretation
OUTER RAMP			
Peloidal intraclast wackestone/packstone	M, K, B	Decimeter- to meter-scale, wavy-bedded recrystallized dolomite mud or very fine peloids with minor angular micritic or silty intraclasts. Scoured bases are common and mudstone partings separate beds.	Distal carbonate deposition via downramp transport of storm remobilized sediment and intraclasts.
Thick-laminated mudstone	M, K, B	Thick-bedded packages of millimeter- to centimeter-scale carbonate mudstone irregular laminae with a few slumps and/or scours. Often strongly petroliferous.	Distal deposition of suspended carbonate fines.
Intraclast breccia	K (rare), M (rare)	Matrix-supported breccias with centimeter- to decimeter-scale, inner-ramp-derived laminated mudstone clasts.	Local debris flows resulting from collapse of local relief on the ramp.
Siliciclastic siltstone	M, K, B	Yellow, pink, or red carbonate-cemented siltstone interbedded with decimeter-scale carbonate beds. Laminae alternate between mixed mineralogy siltstone and clay in thin section.	Pelagic fallout of suspended siliciclastic fines and clay.
MIDDLE RAMP			
Hummocky cross-stratified packstone	M, K, B	Peloid packstone with common hummocky cross-stratification and soft sediment deformation. Smaller beds are often amalgamated into meter-scale packages.	Transport and deposition of fine-grained sediments during storms.
Silty planar-laminated micrite	M, K	Millimeter- to centimeter-scale, uniformly planar-bedded mudstone. Scours, slumps, convolute bedding, and rip-up lenses.	Fallout of suspended fines; subsequent reworking by storm waves.
Black and tan laminite	B	As above with dark organic matter and pyrite-rich laminae alternating with white silty recrystallized limestone. Petroliferous.	Fallout of suspended fines into anoxic environment. Storm wave reworking with variable siliciclastic sediment supply.
INNER RAMP			
Subtidal			
Peloidal to coated-grain grainstone	M, K, B	Well sorted, very fine to fine peloidal to coated-grain grainstone in decimeter-scale beds with abundant tabular and festoon cross-stratification (10 cm [4 in.] wavelength). Mud-draped ripples and a few oncolite grains.	Grainstone barrier shoal complex with constant tidal reworking.
Intraclast dolosiltite	M	Blocky 2–5-cm (0.8–2-in.)-thick beds of fine cream-colored dolomite with large-scale hummocky cross-stratification and self-sourced pebble-size intraclasts. Resedimented ooids in first bed, increasing red silt upward.	Flooding of the platform to a high-energy subtidal environment.

Low-Energy Subtidal to Intertidal			
Oncolite grainstone/ boundstone	M, K	Medium to very coarse oncolite grains (elliptical and 1–5 mm in diameter) in channels and 10–50-cm (4–20-in.)-thick beds with cross-bedding, ripples, and basal scours. Grains have irregularly concentric micritic rims. Few microbial laminations. Heavily silicified.	Coated grains forming in situ in an inner-ramp, wave- and tide-agitated environment. Periods of quiescence allow for microbial binding.
Peritidal Microbialite			
Irregular laminite to stromatolite	M, K	Irregular laminations in peloidal to micritic matrix, common blisters and local relief into centimeter-scale irregular stromatolites. Thick-bedded (dm) or as layers within grainstone facies. Interbedded oncolite grainstone lenses; generally silicified.	Lithified stratiform to domal microbial mats. Local growth of small stromatolites where there is sufficient sustained water depth. Periodic exposure.
Tufted laminite to stromatolite	M, K	Irregular laminations forming tufts with ~1 cm synoptic relief, spaced 3–10 cm. Coated grains fill damp relief.	Organized microbial mat with periodic washover of coarser grains.
Flaser-bedded packstone	B	Fissile centimeter-scale bedded packages of rippled carbonate sand (peloids, ooids, coated grains, oolite fragments, and mudstone chips) and interbedded mudstones; fetid.	Intertidal to subtidal environment with alternating relative high and low wave energy.
Lagoonal Fines			
Mudstone	M, K	Centimeter- to decimeter-bedded, cream-colored carbonate mud, local thin planar laminations.	Restricted shallow pools to lagoons within tidal-flat mosaic.
Laminated dolosiltite	M, K	Silty planar-laminated white carbonate. Local low stromatolites, gypsum lathes, and silt laminae.	Low-energy restricted lagoon.
High-Energy Subtidal to Intertidal			
Mixed grain grainstone/ packstone	M, K	Fine peloids, small oncoliths, ooids, and/or coated grains in centimeter-scale rippled or planar-laminated packages, commonly separated by thin microbial laminite drapes and silicified in bands. Bedding generally 5 to 10 cm (2 to 4 in.) although outsized beds (~50 cm [~20 in.]) occur.	High-energy intertidal grainstone. Local tidal bars or sandwaves.
Smooth-laminated stromatolite	M, K	Meter-scale low synoptic relief domal to conical stromatolites. Elongate in plan view. Laminae are smooth even coats.	Microbial mats forming stromatolites in the lower intertidal zone.
Ooid intraclast grainstone	M, K, B	Spherical to strongly elongate ooids and composite grains with radial fibrous early cements. Intraclasts are composed of mudstone, muddy stromatolite pieces, and resedimented oolite.	High-energy shoal complex formed during large-scale transgression into the Shuram Formation.
Muddy stromatolite	M, K	Up to 2-m (6.6-ft) synoptic relief, 0.5 to 5 m (1.6–16 ft) diameter, bioherms formed from irregular stromatolites with columnar, domal, and conical morphologies all with thick 2 mm (0.08 in.) to 1 cm (0.4 in.) micritic laminae.	Microbial mounds nucleating within the oolite during flooding into the Shuram Formation.

(*continued*)

Table 1. Continued

Facies	Location*	Description	Interpretation
Intertidal to Supratidal			
Fenestral mudstones	K, M	Thin interbedded deposits of mudstone, grainstone, and packstone with evidence of exposure. Grains include fine peloids, coated grains, and oncoids.	Tidal-flat deposits just proximal to the tepee belt.
Tepee breccia	K, M (rare)	Highly deformed sediments and clast-supported in-situ breccia composed of fenestral mudstone to grainstones and/or microbial laminites. Tepee structures are commonly eroded and sometimes capped with red carbonate-cemented siltstone. Beds range in thickness from 10 cm (4 in.) to 2 m (6.6 ft).	Tepees forming in a sabkha environment deforming fenestral mudstone/packstone/grainstone and peritidal microbialite facies. Wind-blown siliciclastics cap zones of prolonged exposure.
Rip-up intraclast conglomerate	M (rare), K	Intraclast conglomerate formed of large (centimeter- to decimeter-scale) clasts of ripped up peloidal grainstone, peritidal microbialite, and/or mudstone in grainstone matrix. Commonly imbricated.	Storm-wave transport of reworked early cemented peritidal sediments.
Siliciclastic Influenced			
Calcarenite to quartzarenite	B	Cross-bedded fine to medium, subrounded to rounded, often fractured quartz sand mixed in various percentages with carbonate mudstone chips and intraclasts, ooids, reworked oolite, coated grains, and peloids; calcite cemented.	Intertidal marine sand proximal to a siliciclastic source incorporating carbonate grains and resedimented carbonate.
Quartz sandstone	M, K	Well-rounded quartz sand in lenticular bedsets, with tabular, herringbone, planar, and low-angle stratification, frequently bidirectional. Carbonate intraclast lags are common at the base. Limited spatial extent at outcrop scale.	Tidal channels cutting through inner-ramp facies.

*M = Mukhaibah dome; K = Khufai dome; B = Buah dome.

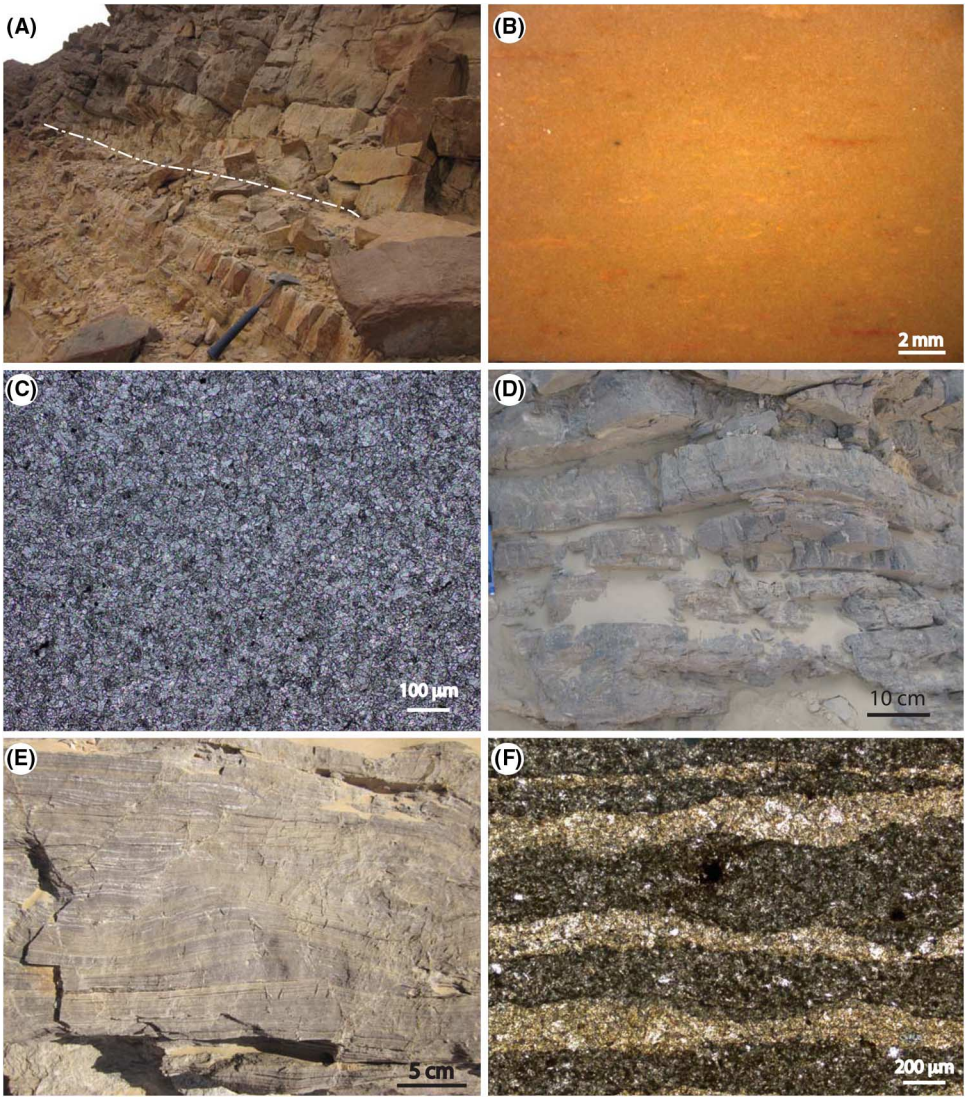

Figure 6. Outer and middle ramp facies tracts. (A) Contact between Masirah Bay and Khufai Formations in at KDS2, hammer is 32 cm (12.6 in.) tall. (B) KDS2 0.7 intraclast wackestone slab from the section base. (scale in millimeters). (C) Photomicrograph of MD5 0.1 very fine recrystallized dolomite. (D) Hummocky cross-stratification from KDE section (pencil is 15 cm [6 in.]). (E) Planar-laminated mudstone facies are MDE. (F) Photomicrograph of BD1 244.5 black and tan laminite showing dark silt-rich laminae interbedded with more coarsely crystalline, cleaner calcite.

recrystallization generally obscures primary clast and matrix components. The intraclast breccia facies was interpreted as evaporite collapse breccias (Gorin et al., 1982) and as slope collapse breccias (McCarron, 1999). Given their lateral equivalence with subwave base intraclast wackestone facies, we suggest that they record debris flows of slope materials on the distal ramp. These deposits are very rare in all sections and do not create the laterally continuous facies belt characteristic of steep-sided platform margins (Read, 1985).

Siliciclastic Siltstone

Siltstones interbedded with dolomite at the Khufai-Masirah Bay transition correspond to the siltstone component of facies E2 described in Allen and Leather (2006) (Figure 6A). Beds are 5–20 cm (2–8 in.) thick, separating larger packages of fine-grained carbonate. Siltstone is interpreted to have been deposited below wave base by settling of suspended sediment.

Middle-Ramp Facies Tract

The middle-ramp facies tract consists of hummocky cross-stratified peloidal packstone and silty planar-laminated mudstone and records the slow progradation of the early highstand systems tract (HST) after the MFI. It is distinguished from the outer-ramp facies tract by containing storm-generated sedimentary structures, including increased evidence of wave reworking.

Hummocky Cross-Stratified Peloidal Packstone

Hummocky cross-stratified peloidal packstone is composed of fine peloids with hummocky cross-strata, slump structures, and convolute bedding amalgamated in meter-scale packages (Figure 6D). It alternates with peloidal intraclast packstone and caps depositional cycles. Dolomitization obscures primary grain boundaries. The onset of storm reworking, gradual increase in grain size, and stratigraphic position suggest the hummocky cross-stratified cross-bedded packstone and grainstones represent progradation of the ramp sequence. The amalgamated packages of hummocky cross-stratified packstone are interpreted as the product of storm wave activity.

Silty Planar-Laminated Mudstone

Strikingly planar-laminated silty mudstone (Figure 6E) contains millimeter- to centimeter-scale very even laminations, with a few small-scale scours, slumps, and self-sourced imbricated intraclast conglomerate. This unit overlies the hummocky cross-stratified sections and directly precedes the transition to the inner-ramp facies in all domes. This facies is similar to the rhythmically interbedded limestone-argillite facies described from the Mississippian of Wyoming and Montana (Elrick and Read, 1991), albeit without evidence for burrowing. The lack of evidence for desiccation or frequent wave action, combined with evidence for quiet water suspension fallout with local storm reworking, is consistent with the middle-ramp environment. The production of rigid clasts from these laminae suggests a degree of early cementation not observed in the deeper water facies.

Black and Tan Laminite Subtype (Buah Dome Only)

At the Buah dome, the silty planar-laminated mudstone facies is a distinctive dark-gray and tan, strongly petroliferous, planar laminite (Figure 6F). Beds are 1–3 m (3.3–10 ft) thick and extended the entire length of the outcrop area (5 km; 3 mi) and exhibit both plastic and brittle small-scale deformation. The depositional environment of these laminites is interpreted to be physically similar to that of the silty laminites described above. However, the relative plasticity and cohesion of laminae clasts indicate less extensive early cementation, and strong organic and pyrite components visible in thin section suggest a low-oxygen environment.

Inner-Ramp Facies Tract: Subtidal

The inner-ramp subtidal facies tract consists of peloidal to coated grainstone and intraclastic dolosiltite. These two facies appear in distinct parts of the depositional sequence: first, as the facies shallow during the highstand, and second, as the ramp is flooded during transgression associated with the upper formation boundary. They are grouped here because they represent a similar sediment supply, wave energy, and water depth, consistent with the concept of a facies tract (Kerans and Fitchen, 1995).

Peloidal to Coated Grain Grainstone

The peloidal to coated grain grainstone facies is the first unambiguous appearance of extensively cross-bedded grainstone within the facies succession (Figure 7A). This light-gray to white peloidal dolomite occurs in decimeter-scale discontinuous beds. Grains are fine micritic peloids with or without a coating of micritic cement, with larger grains congregating in ripple troughs. The appearance of peloidal grainstone is abrupt across the Huqf area, indicating shoaling of the platform to fair-weather wave base and forming a 15- to 25-m (49- to 82-ft)-thick stratigraphic band that is laterally continuous with minor interfingering of facies stratigraphically from above and below. This transition is frequently coeval with a formation-scale visual character change from dark-gray and petroliferous facies below to buff colored above (Figure 4A). This facies is commonly poorly exposed, coinciding with the level of the Tertiary-age peneplanation surface and associated silcrete breccias.

Intraclast Dolosiltite

Intraclast dolosiltite occurs as a 2-m (6.6-ft)-thick package at the Khufai-Shuram boundary at the Mukhaibah dome. It consists of thin swaley-bedded cream to pink dolosiltite that includes increasing amounts of red siliciclastic silt upward in the package (Figure 7B). Ripped up pebble-size clasts of this facies are preserved as thin intraclast conglomerate beds. The dolosiltite beds onlap stromatolitic

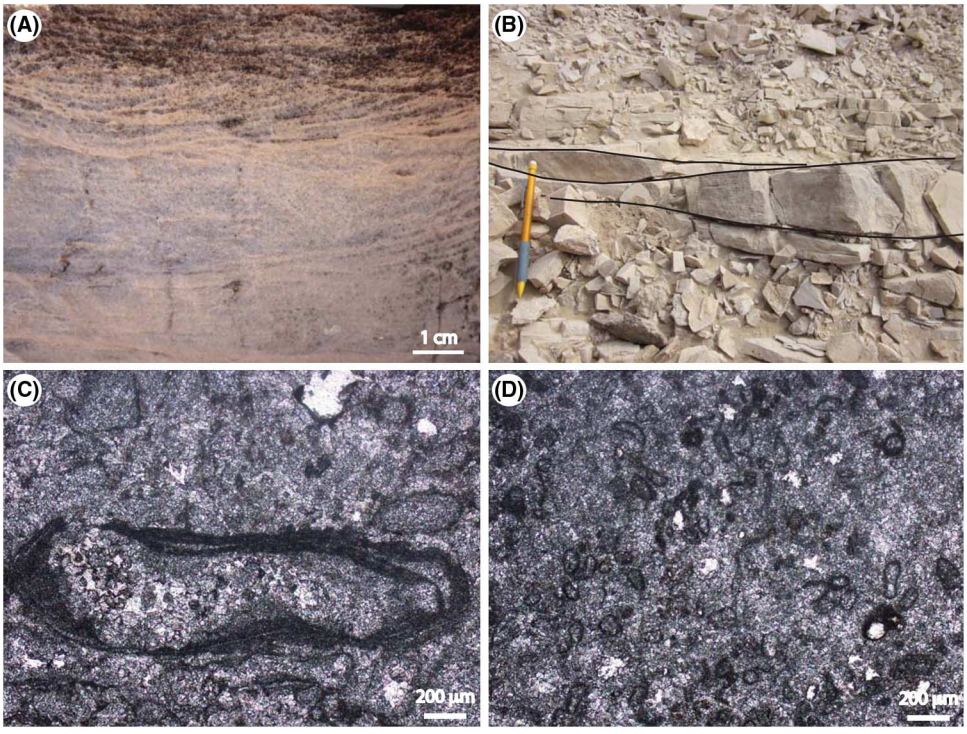

Figure 7. Inner-ramp subtidal and intertidal grainstone facies. (A) KDS 114.4, festoon cross-bedding in peloidal to coated grainstone facies. (B) MDE, intraclast dolosiltite facies in outcrop showing hummocky cross-stratification and blocky bedding. Contact with the Shuram Formation is in the rubble at the top of the photograph. Pencil is 15 cm (6 in.). (C) MD5 152.0 photomicrograph, large oncolite grain in finer peloidal matrix from oncolite grainstone/boundstone facies. (D) MD5 131.5 photomicrograph, fine-coated grains and peloids.

bioherms on the underlying bedding surface (see below). This facies is interpreted to record an abrupt deepening of the platform during the large-scale transgression into the Shuram Formation, recording high-wave-energy events in a subtidal setting. Increasing silt content with stratigraphic height marks the transition into the lower Shuram Formation.

Inner Ramp: Variable-Energy Subtidal to Intertidal

The variable-energy subtidal to intertidal facies tract is a diverse group and includes oncolite grainstone to boundstone, peritidal microbialite (tufted and irregular), flaser-bedded peloidal packstone, and lagoonal mudstone and dolosiltite deposits. These facies are distributed within the peritidal part of the Khufai Formation, beginning above the first grainstone shoals.

Oncolite Grainstone to Boundstone

Oncolite grainstone consists of thick cross-bedded, channelized packages of oncoids and coated grains. Large oncoids (up to 5 mm [0.2 in.]) occur in channels and bed bases and are elliptical with crinkly micritic rims commonly showing multiple concentric, although irregular, rings (Figure 7C). Microbial laminae bind oncoids within some beds, forming boundstone facies. These facies are commonly heavily silicified with near-complete replacement of carbonate.

Although oncoids are described from a variety of depositional environments (Tucker and Wright, 1990), a shallow, wave-agitated origin for this facies is suggested by the context presented here. Sedimentary structures indicate wave (or tidal) reworking; however, binding by microbial laminae suggests periods of quiescence. The oncoid grains themselves suggest a similar genesis because the irregular coatings are indicative of colonization by microbial mats, but roundness of grains suggests at least periodic rolling (see discussion in Tucker and Wright, 1990). This facies is similar to the ooid and oncolite shallow ramp carbonate of the Upper Cambrian Nolichucky Formation described by Markello and Read (1981). In that setting, the carbonate sands formed a barrier between cyclic peritidal deposits of the shallow inner-ramp and deeper subtidal deposits (Markello and Read, 1981).

Peritidal Microbialite

Peritidal microbialite forms a subgroup of the variable-energy subtidal to intertidal facies tract and consists of tufted laminites, irregular laminites, and stromatolites. These microbial textures are intimately associated with one another and frequently grade laterally and vertically within the same bed. The term stromatolite is applied in cases where the synoptic relief formed by laminae is more than a few centimeters. Irregular laminite is defined by irregular micritic laminae with no systematic higher order structure, occurring both as thick-bedded units (Figure 8A) and as thin layers within oncolite or peritidal grainstones (see below). Laminae are irregular to convolute and trap pockets of coated grains (Figure 8B). Tufted laminite is similar, but the laminae form small tufts that show a high degree of inheritance, extending upward through beds at decimeter scale, although the synoptic relief at any given time was probably less than 1 cm (0.4 in.) (Figure 8C). Tufts are dampened where carbonate grains accumulate in troughs and are coated by the subsequent laminae (Figure 8D). Tufts can form the nuclei of small (3–10 cm; 1.2–4 in.) conical stromatolites. Both laminite types tend to be heavily silicified and commonly show evidence for intermittent subaerial exposure including blisters, mudcracks, tepees, and in-situ breccias.

We interpret the peritidal microbialite facies group as formed by the preservation of microbial mats in the shallow intertidal zone. The carbonate accumulation likely occurred through a combination of trapping and binding (where grains are visible) and direct precipitation of carbonate (Fairchild, 1991). Microbial laminite commonly caps facies of the subtidal and intertidal parasequences and parasequence sets. Distribution of desiccation structures confirms these shallowing-upward trends. Primary porosity was occluded by early silicification.

Flaser-Bedded Packstone

Flaser-bedded packstone occurs at the Buah dome at the equivalent stratigraphic interval of microbially influenced sedimentation elsewhere. Here, laminae to thin beds of rippled fine carbonate sand (grains primarily include peloids and resedimented carbonate mud) alternate and are draped by carbonate and siliciclastic mud (Figure 8E) with no evidence of desiccation. Significant recrystallization forms coarse calcite spar that obscures primary fabrics within this facies. Flaser-bedded packstone beds commonly are associated with black and tan laminites; in one location, a parasequence composed of these facies is capped by irregular laminite. This sequence defines a shallowing-upward package, suggesting that the flaser-bedded packstone formed in an intertidal depositional environment. Similar flaser-bedded ribbon rocks were described from South China and interpreted as tidal-flat deposits (Lehrmann et al., 2001). However, the lack of desiccation features here suggests a deeper water setting with variable energy more similar to the ribbon rock carbonates described from the Middle Cambrian of Virginia (Koerschner and Read, 1989).

Lagoonal Fines

The lagoonal fines facies includes mudstone and laminated dolosiltite and represents low-energy, deeper water parts of peritidal cycles in the Khufai Formation. Mudstone is buff or white colored occurring in thinly bedded packages with no visible grain character or evidence for wave reworking. Very even planar lamination and thin irregular laminae occur in some beds. Laminated dolosiltite occurs regularly as parasequence bases and is defined by bright white packages of even thinly bedded to laminated dolosiltite with intercalated beds of carbonate-cemented silt (Figure 8F). Silicified beds contain evaporite molds, but no evidence of exposure is observed. Very low domal structures interpreted as stromatolites formed in a few intervals.

The origin of Precambrian mudstone is debated with possible explanations ranging from direct precipitation from the water column, precipitation as stromatolite laminae and subsequent disaggregation, or disintegration of algal skeletons similar to today (Grotzinger, 1989; Knoll and Swett, 1990; Tucker and Wright, 1990; Fairchild, 1991; Sumner and Corcoran, 2001; Dibenedetto and Grotzinger, 2005). Large accumulations of mudstone occur in Proterozoic carbonate platforms in a variety of depositional environments (Grotzinger, 1986a, 1989; Knoll and Swett, 1990; Sami and James, 1994,

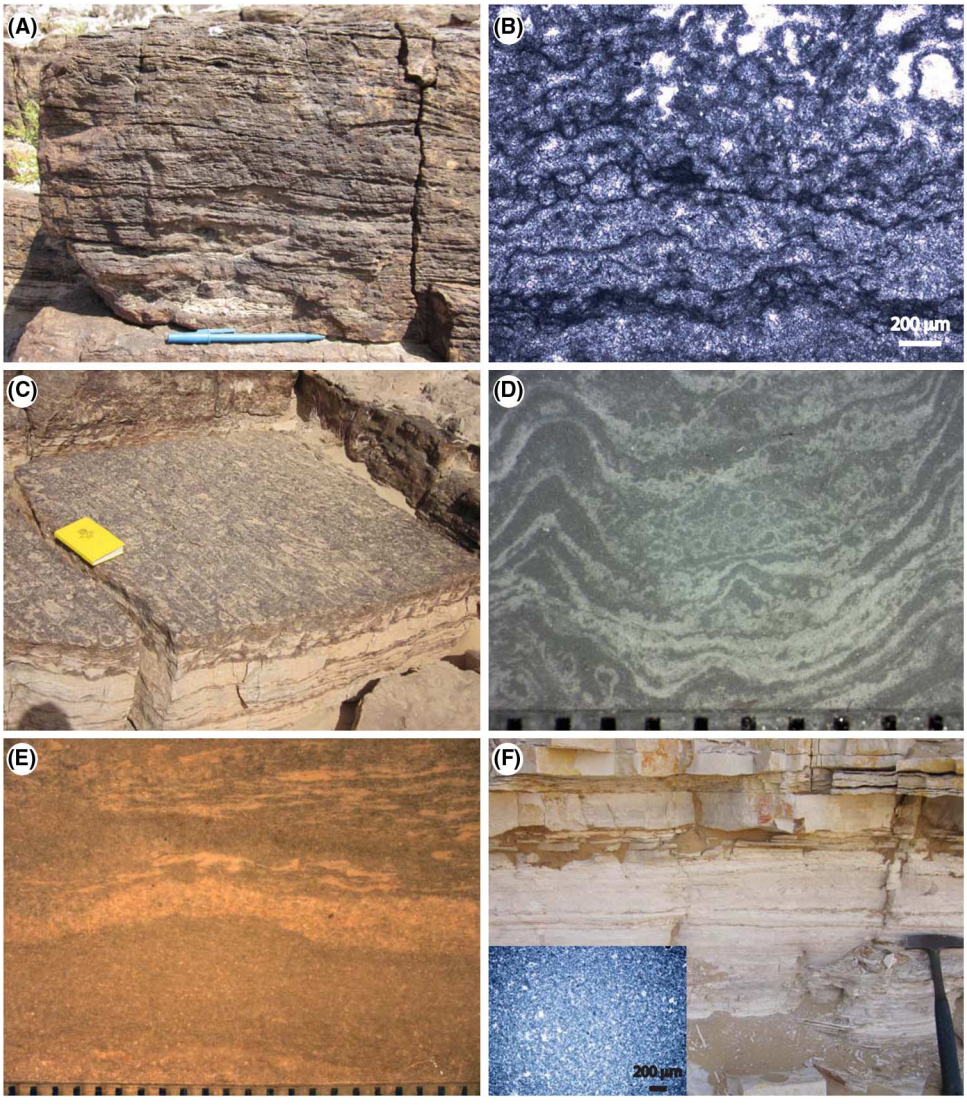

Figure 8. Peritidal microbialite and inner ramp. Subtidal facies (A) thick bed of irregular laminite. Pen is 16 cm (6.3 in.). (B) KDW2 21.9 photomicrograph of irregular micritic laminae in both thick laminae and coating and binding grains. (C) Plan and side view of tufted laminite bed showing parallel tuft crests. Notebook is 19 cm (7.5 in.) tall. (D) MDE 122 photomicrograph, tufted laminite with coated grains damping tuft topography. Scale is in millimeters. (E) BD5 flaser-bedded packstone facies in slab. Scale is in millimeters. (F) Laminated dolosiltite in outcrop. Hammer is 32 cm (12.6 in.) long. Inset is a photomicrograph of a similar material from the Khufai dome.

1996). The sedimentary features described here are consistent with fallout of suspended or precipitated fines in a protected, low-energy environment such as a backshoal lagoon. The lack of sedimentary structures, planar lamination, and stratigraphic context of dolosiltite facies also suggests a restricted lagoonal environment. This is similar to the thick-laminated dolosiltite described by Grotzinger (1986a) in the Rocknest Formation of northwest Canada. Sedimentary structures are more limited in the Khufai Formation example, but this could be attributed either to a more protected environment or a deeper lagoon. Evaporite laths suggest a hypersaline porewater composition at least periodically during deposition.

Inner Ramp: High-Energy Subtidal to Intertidal Facies Tract

The high-energy subtidal to intertidal facies tract consists of mixed grain packstone and grainstone, smooth laminated stromatolite, oolitic intraclast grainstone, and stromatolite bioherm facies. The former two facies comprise a large proportion of peritidal deposits, where the latter two are characteristic of the transgressive surface of the uppermost Khufai Formation.

Mixed Grain Grainstone and Packstone (Peritidal Grainstone)

The mixed grain grainstone and packstone facies is composed of fine wave-reworked heterolithic

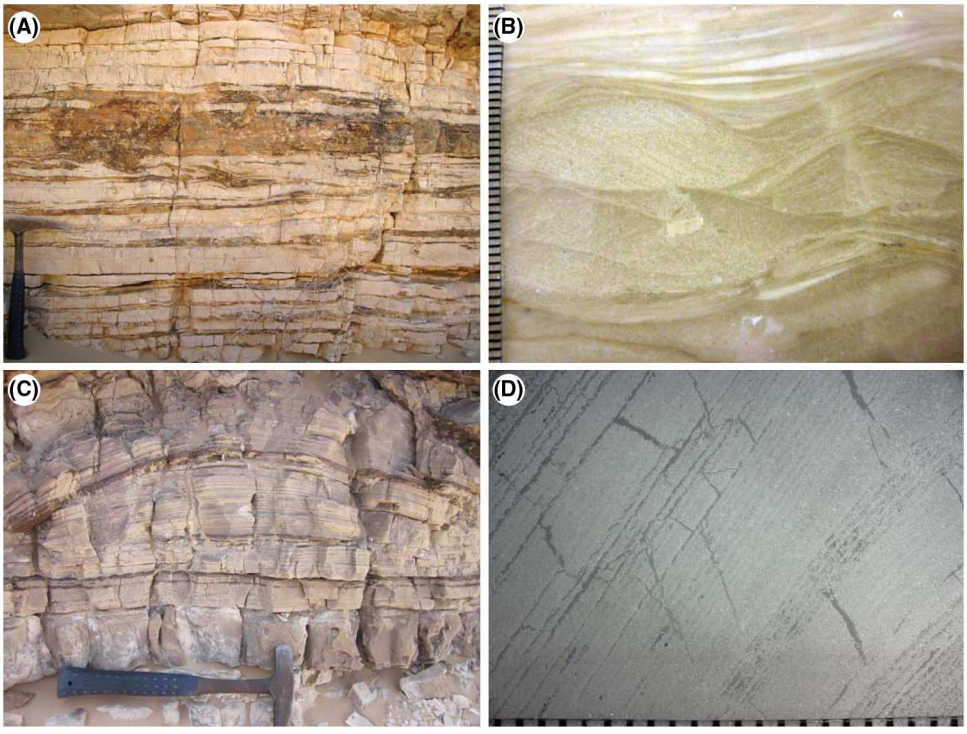

Figure 9. Inner ramp: high-energy facies. (A) Peritidal grainstone facies in outcrop at KDW, hammer is 32 cm (12.6 in.) tall. (B) NA1 1.4 slab, ripple cross-laminated coated grain to ooid grainstone. Scale in millimeters. (C) KDS 264 outcrop, Low domal stromatolite. Hammer is 32 cm (12.6 in.) tall. (D) MD6 174 thin-section, smooth laminated stromatolite. Scale is in millimeters.

grainstone and packstone and can contain interbeds of many different facies, including irregular laminite, intraclast conglomerate, and local mudstone (Figure 9A). Ooids occur rarely and primarily at the Mukhaibah dome. Sedimentary structures include current ripples, climbing wave ripples (Figure 9B), small dunes, and mudcracks. Granular composition and sedimentary structures in the mixed grain grainstone and packstone facies indicate a high-energy intertidal environment (Tucker and Wright, 1990). Carbonate sands were deposited where wave and tidal energy was high and were then colonized by microbial communities and/or draped by mud during periods of quiescence. The outsized beds of similar composition may represent local tidal bars or sand waves.

Smooth-Laminated Stromatolite

The smooth-laminated stromatolite facies includes a variety of morphologies with a common fine and even lamination style (Figure 9C, D). Stromatolitic beds form continuous sheets and are nucleated on rippled peritidal grainstone beds. Elliptical, laterally linked domes are the most common morphology and range in size from 20 cm (8 in.) to several meters across (Figure 9C). Other morphologies include columns, cones, and domes. Morphologies grade laterally and vertically into one another. This gradation is interpreted to represent local variability in wave energy and sediment supply as is noted in the modern examples at Shark Bay, Australia (Tucker and Wright, 1990; Grotzinger and Knoll, 1999). The smooth laminated texture suggests formation via precipitation onto the surface of microbial mats instead of trapping and binding of carbonate clasts by mats. Water depth is likely related to the synoptic relief of any given stromatolite, probably in these cases ranging from shallow intertidal to subtidal for the largest examples (e.g., Grotzinger, 1986b; Fairchild, 1991; Riding, 2000).

Ooid-Intraclast Grainstone

Although ooid grainstone is rare through most of the Khufai Formation, the uppermost TST is oolite rich. In particular, a distinctive bed of coarse intraclast ooid grainstone occurs everywhere the contact with the Shuram Formation is preserved in the Huqf (Figure 10A). Additionally, oolites are common in the upper 35 m (115 ft) of the Buah dome sections.

Ooid grainstone beds are cross-bedded with structures, including large-scale bar forms, tabular

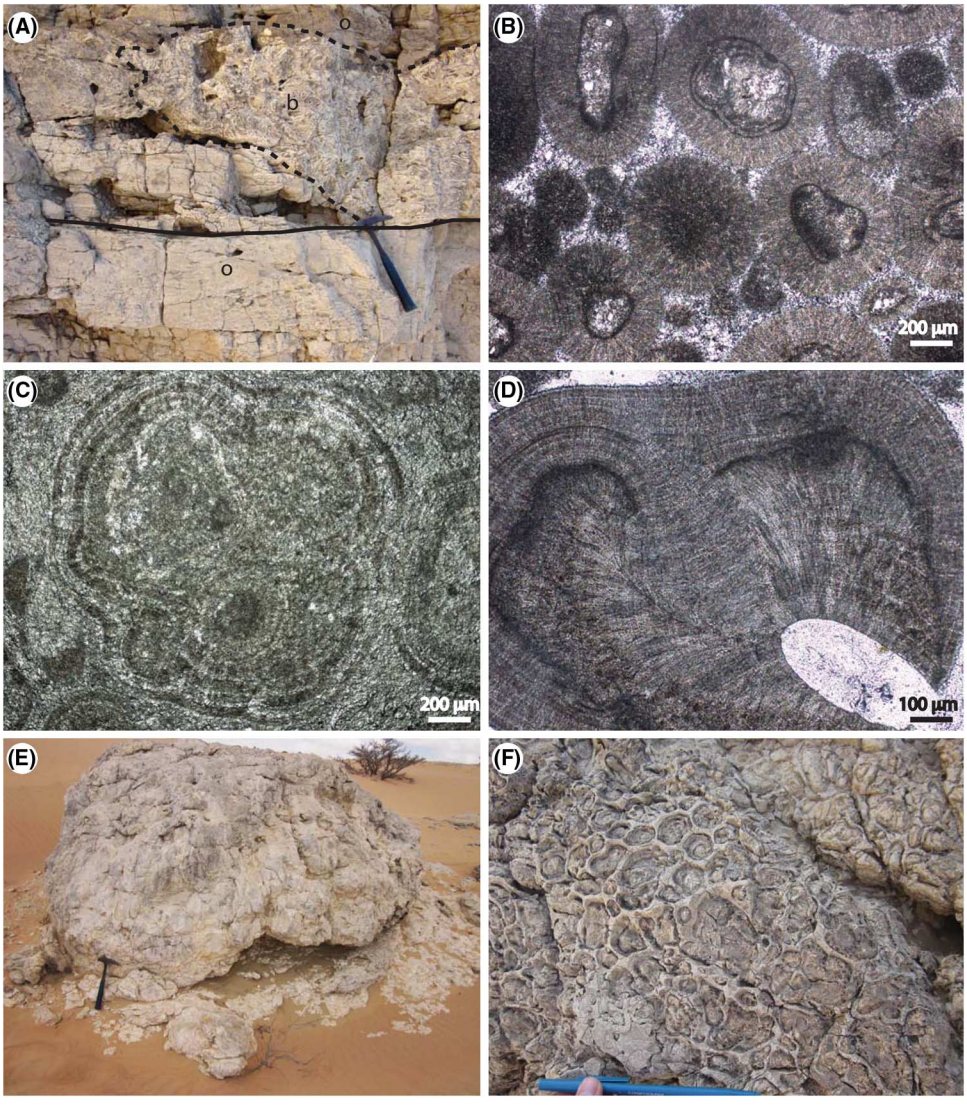

Figure 10. Inner ramp: high-energy (transgressive) facies. (A) Oolite bed in outcrop at MDE. Hardground outlined in solid line, stromatolite bioherms outlined in dashed line (b), and oolite indicated by (o). Hammer is 32 cm (12.6 in.) tall. (B) MD5 309.5 photomicrograph, ooid grainstone showing radial fabric. (C) KDW2 131.5 photomicrograph, composite grain composed of small ooids with multiple exterior concentric coats. (D) MD6 258.7, ooid detail showing plumose interior recrystallization and radial exterior fabric. (E) KDW2 UPK10, large micrite stromatolite bioherms in outcrop at the Khufai-Shuram boundary. Hammer is 32 cm (12.6 in.) tall. (F) Detail of stromatolite bioherms at MDE showing small silicified stromatolites and surrounding matrix; pen is 16 cm (6.3 in.) long.

cross-beds, and ripples. Grain morphologies include spherical ooids, coated elongate clasts, and composite coated grains. In contrast to the oncoliths and coated grains that occur stratigraphically lower, these ooids show radially concentric crystal orientation along with distinctive plumose cement in ooid interiors (Figure 10B, D). Intraclasts are concentrated as lags and contain stromatolite laminae, mudstone, or cemented oolite clasts. A hardground is preserved within the oolite bed at the Mukhaibah dome (Figure 10A). We interpret the ooid-intraclast grainstone facies to have formed in a high-energy shoreface to shoal environment. The large cross-bedding in the northern Khufai dome was previously interpreted as tidal bars (Le Guerroue et al., 2006a), and other sedimentology is consistent with modern and ancient ooid shoal deposits (Wilson, 1975). Intraclasts appear to derive primarily from coeval stromatolites and cemented oolite.

Muddy Stromatolite

The muddy stromatolite facies is an unusual stromatolite morphotype that differs from previous examples both in lamination style and gross morphology and are syndepositional with the ooid-intraclast facies described above. Laminae are thick microcrystalline micrite, with ooids incorporated between muddy laminae. The stromatolites form large isolated bioherms with up to 2 m (6 ft) of synoptic relief (Figure 10E). The stromatolitic subunits alternate between irregular

clusters of small columns (Figure 10F) and thick continuous laminae. The stromatolites nucleate along a hardground within the upper oolite bed and are onlapped by the intraclast dolosiltite facies and lowermost Shuram Formation.

Inner Ramp: Intertidal to Supratidal

The intertidal to supratidal facies tract consists of fenestral (mixed-grain) mudstones, tepee breccia, and rip-up intraclast conglomerate and is characterized by evidence for periodic to prolonged subaerial exposure.

Fenestral Mudstones

The fenestral mudstones facies is a mixed facies group of mudstones, wackestones, and packstones united by close sedimentary proximity and evidence of exposure and/or very shallow-water depositional conditions. Sediment types are interbedded in thin-bedded packages that commonly are deformed by tepee structures. Millimeter-scale subspherical to lozenge-shaped horizontal fenestrae and tabular, vertically oriented, crystal molds resembling gypsum laths are very common (Figure 11A). Primary evaporite minerals forming lath structures were replaced with silica (Gorin et al., 1982; Wright et al., 1990). Grains are similar to those in the previous facies tract, and sedimentary structures include mudcracks, low-amplitude wave ripples, and tepee structures. In concurrence with previous interpretations (Wright et al., 1990; McCarron, 1999), this facies is interpreted to have formed on a shallow intertidal to supratidal flat. In contrast to the observations of Wright et al. (1990) who note a paucity of mud, we observe significant accumulations of muddy matrix within these deposits, consistent with the sedimentology of modern tidal flats (Shinn et al., 1969).

Tepee Breccia

Tepee structures are ubiquitous in the upper 100 m (330 ft) of the Khufai Formation at the Khufai dome and occur uncommonly at the Mukhaibah and Buah domes. Tepees grade from mild upwarping (Figure 11B) to extensive breccias (Figure 10C) (Kendall and Warren, 1987) and form meter-scale polygonal fractures across exposed bedding planes. Tepees primarily deform fenestral mudstone facies; however, peritidal microbialite and grainstone facies also are affected. Cementation is extensive and includes calcite rim cements and coatings on breccia clasts, calcite spar in vugs, and silica replacement. Vadose pendant cements and large pisoids commonly associated with tepee structures in other locations are not observed in the Khufai Formation (Assereto and Kendall, 1977; Kendall and Warren, 1987). Thin beds of red siltstone are locally preserved on the upper surface of tepee breccia deposits.

The tepee breccia facies is interpreted to have formed in a very restricted sabkha environment and indicates periodic subaerial exposure. Where tepee peaks are eroded or the breccias are most well developed, significant depositional hiatuses very likely occurred. At the Khufai dome, multiple parasequences of meter-scale tepees are superposed forming an amalgamated, highly restricted parasequence set (e.g., Grotzinger, 1986b). The concentration of these features at the Khufai dome suggests that these outcrops are the most proximal exposures of the Khufai Formation.

Rip-Up Intraclast Conglomerate

Rip-up intraclast conglomerates are formed of coarse imbricated tabular intraclasts scoured from underlying beds in a coated grain to coarse oncoid grain-dominated matrix (Figure 11D). At the Khufai dome, beds are laterally extensive and, in some cases, can be correlated for 10 km (6 mi) or more. The regionally extensive character and clast imbrication above scoured surfaces suggest that these beds were deposited when storm-generated currents eroded the inner ramp. The matrix derives from adjacent grainstone facies tracts, where large intraclasts were scoured and deposited locally. This facies is equivalent in origin to the regionally extensive intraclast packstone facies (e.g., Grotzinger, 1986b).

Inner-Ramp Facies Tract: Siliciclastic Influenced

The siliciclastic-influenced facies tract consists of mixed calcarenites to quartzarenites and quartz sandstone facies. Siliciclastic sediments occur only locally

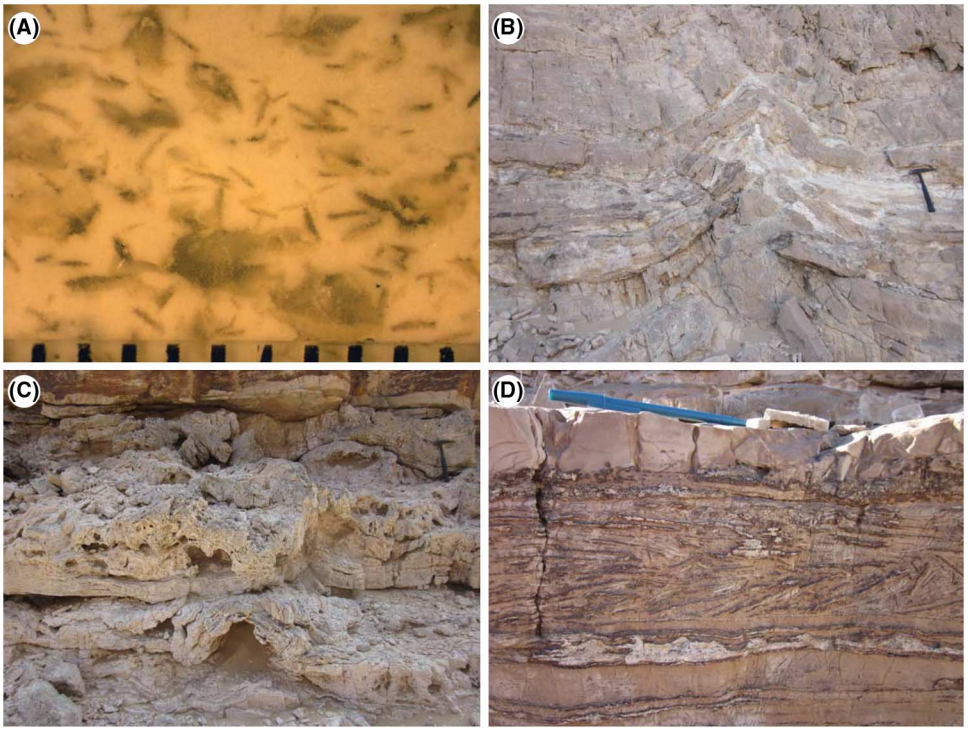

Figure 11. Inner ramp: Intertidal to supratidal facies. (A) MDE, fenestral mudstone slab with evaporite lathes of multiple morphologies. Scale is in millimeters. (B) Khufai dome (DG) outcrop, large immature tepee. Hammer is 32 cm (12.6 in.) tall. (C) KDW2 32 outcrop, multiple sets of heavily deformed tepees in fenestral mudstone. Hammer is 32 cm (12.6 in.) tall. (D) Khufai dome (PF1) outcrop, silicified imbricated intraclast conglomerate. Pen is 16 cm (6.3 in.) long.

at the Khufai and Mukhaibah domes, whereas all sections at the Buah dome feature mixed carbonate-siliciclastic sediments beginning approximately 90 m (295 ft) from the basal contact. This change in sediment type warrants a new facies tract.

Calcarenites to Quartzarenites

The calcarenite to quartzarenite facies contains medium- to thick-bedded carbonate-cemented sandstone with a variable proportion of carbonate grains. Extensive scouring and cross-bedding occur in most packages (Figure 12A). Carbonate-rich and sand-rich beds are intimately associated with each other and alternate at a fine scale with sand grains even serving as the nucleus for carbonate coatings (Figure 12B). Carbonate mud is the matrix in both quartz- and carbonate-dominated beds.

During deposition, quartz sand grains were transported into a zone of carbonate production. A modern analog for this area is the mixed carbonate-siliciclastic deposition occurring in estuaries of the Great Barrier Reef, Australia. Here, relatively coarse quartz sands are incorporated into variably muddy to grainy shallow-marine sediments with sediment distribution controlled by local coastline and reef geometries (Orpin et al., 2004). The river system supplying siliciclastics into the underlying Masirah Bay Formation was hypothesized to be located to the north of Huqf exposures (Allen and Leather, 2006), consistent with the northern location of the Buah dome.

Quartz Sandstone

Up to four packages of carbonate-cemented quartz sandstone occur in the upper Khufai and Mukhaibah domes. These packages are 1–3 m (3.3–10 ft) thick and extensively cross-bedded (Figure 12D). Large (centimeter- to decimeter-scale) clasts of underlying carbonate beds occur as basal lags. Grains are fine- to medium-size, well-sorted quartz sand. We differentiate this facies based on the high quartz content, cross-bedding, and lack of lateral continuity. Bidirectional cross-bedding suggests a tidal influence on these sediments, and the scouring relationships and bed geometries suggest migrating channels. This facies was interpreted as southward extensions of tidal channels sourced from the Buah dome area (McCarron, 1999). We concur with the tidal channel interpretation; however, note that this facies occurs stratigraphically above the main sand bodies at the Buah dome.

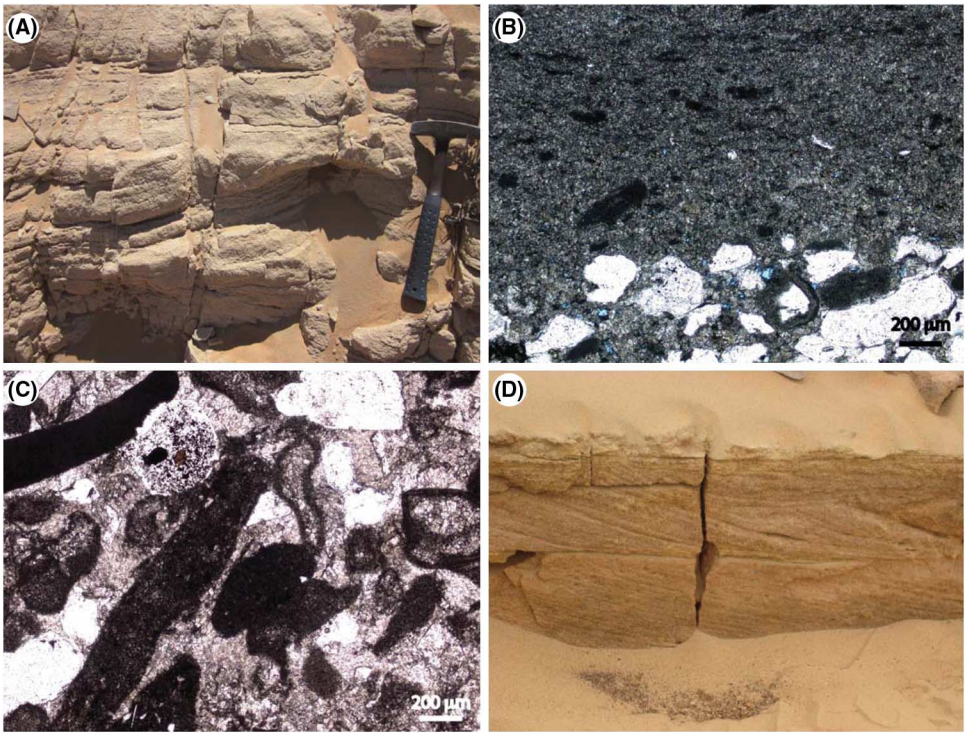

Figure 12. Sand-containing facies. (A) BD6 45 cross-bedded quartz sand in outcrop at the Buah dome. Hammer is 32 cm (12.6 in.) long. (B) BD1 106.3 photomicrograph, intraclast wackestone interbedded with carbonate rich quartz sandstone. (C) BD1 164.5 photomicrograph, primarily carbonate grainstone with micrite and coated grains with inclusion-rich quartz sand, calcite cement. (D) KDW2 upper sandstone in outcrop showing tabular planar cross-bedding in quartz sand. Bed is approximately 20 cm (4 in.) thick.

FACIES AND FACIES TRACTS: OMAN MOUNTAINS

The Khufai Formation exposed in the Oman Mountains comprises two main facies tracts: transitional and carbonate dominated (Table 2). The former is siliciclastic dominated and occurs at the Masirah Bay-Khufai and Khufai-Shuram Formation boundaries. Because the transitional facies are genetically related to the rest of the Khufai Formation, they are included in our discussion. The carbonate-dominated facies tract varies considerably in thickness ranging from 20.1 m (65.9 ft) at the Al Aqor section to 122.5 m (401.9 ft) at Wadi Hajir. Thickness variation corresponds to bed thickness, suggesting a relationship with the supply of carbonate material. Significant postdepositional folding and faulting prevents quantitative analysis of the depositional distance between these sections.

Transitional Facies Tract

The transitional facies tract consists of siliciclastic siltstone, crinkly laminite, and intraclast wackestone. The lower transition begins at the first major carbonate bed within the upper Masirah Bay Formation siltstone. Carbonate facies alternate with siltstone over a thickness of 10 to 30 m (33 to 100 ft) before an abrupt transition to carbonate-dominated facies. The upper transition begins at the termination of the main body of carbonate deposition and is marked by a 1-m (3.3-ft)-thick bed of red siltstone after which marl and crinkly laminite alternate with siltstone. Quartz sand beds also punctuate the upper transition in some sections.

Siliciclastic Siltstone

Siltstone is volumetrically the largest component of the transitional facies tract and is tan, white, or pink in outcrop, with thin crinkly laminations (Figure 13A). This facies was interpreted to record settling of fines from suspension in deep water (Allen and Leather, 2006).

Thick-Bedded Intraclast Wackestone

The thick-bedded intraclast wackestone facies occurs in discontinuous beds 0.5 to 2 m (1.7 to 6.6 ft) thick. The matrix is composed of gray, silty lime-mudstone with small siltstone intraclasts concentrated at bed bases. Bed thickness, intraclast entrainment, and composition suggest that these beds represent periodic transport of carbonate from higher on the ramp

Table 2. Facies and Facies Tracts of the Khufai Formation: Oman Mountains

Facies	Description	Interpretation
Transitional Facies Tract		
Siltstone	Pink to white laminated silt in centimeter-scale beds.	Suspension settling from siliciclastic source.
Crinkly laminite	Dark-gray to black fetid carbonate with subordinate silt. Decimeter- to meter-scale beds (lensoidal) containing very thin crinkly laminations. Rollup structures common, but no evidence for wave agitation, exposure, or phototaxis.	Benthic microbial mat subject to gravitational slumping or infrequent storm waves.
Thick-bedded intraclast wackestone	Massive decimeter- to meter-scale lensoidal beds. Chips of carbonate suspended in very fine peloidal mudstone.	Mass-flow deposits from zone of carbonate production.
Carbonate-Dominated Facies Tract		
Graded intraclast wackestone and packstone	Black fetid limestone with bedding generally between 4 and 20 cm (1.5 and 8 in.) thick (2 to 40 cm [0.8 to 16 in.] total range) Angular very fine to fine dolomite grains graded in lime mud or very fine peloidal matrix. Scours and dewatering structures are common.	Deposition from turbidity currents off of the upper ramp.
Coarse-graded grainstones	Rounded tan dolomite pebbles graded in wackestones deposits. Common evidence of multiple generations of flow and microbial coatings.	Coarse deposition in area otherwise bypassed by fine sediments.
Lime mudstone	Light-gray massive centimeter-scale mudstone beds. Generally deformed under subsequent turbidite flows.	Suspension fallout of fine pelagic carbonate.
Graded grainstone	Degraded ooids, peloids, and dolomicrite grains. Graded bedding but no sedimentary structures.	High-energy, turbidity current, subwave base deposition.
Slumped quartz sandstone	Fine to medium quartz sand with carbonate intraclasts. Exhibits extensive soft sediment deformation.	Sand being shed from tidal channels on the upper-ramp area.

into the basin by sediment gravity flows. As the flows moved across siltstone beds, they were reworked to provide intraclasts.

Crinkly Laminite

The crinkly laminite facies is dark gray to black and occurs both as coherent beds (10–50 cm [4–20 in.]) or capping thick intraclast wackestone beds (Figure 13A). Small-scale plastic deformation of the crinkly laminite is common and includes small folds and roll-up structures. Crinkly laminites are uncommonly well preserved. The fabric consists of very fine, crinkly, silty, carbonate mud laminae separating pockets of calcite sediment (Figure 13B). The irregular texture and plastic deformation of the crinkly laminite facies suggest binding cohesion of microbial mats. The lack of physical abrasion, lack of evidence for phototaxis, and the facies association within which crinkly laminite facies occur suggest a deep-water depositional environment.

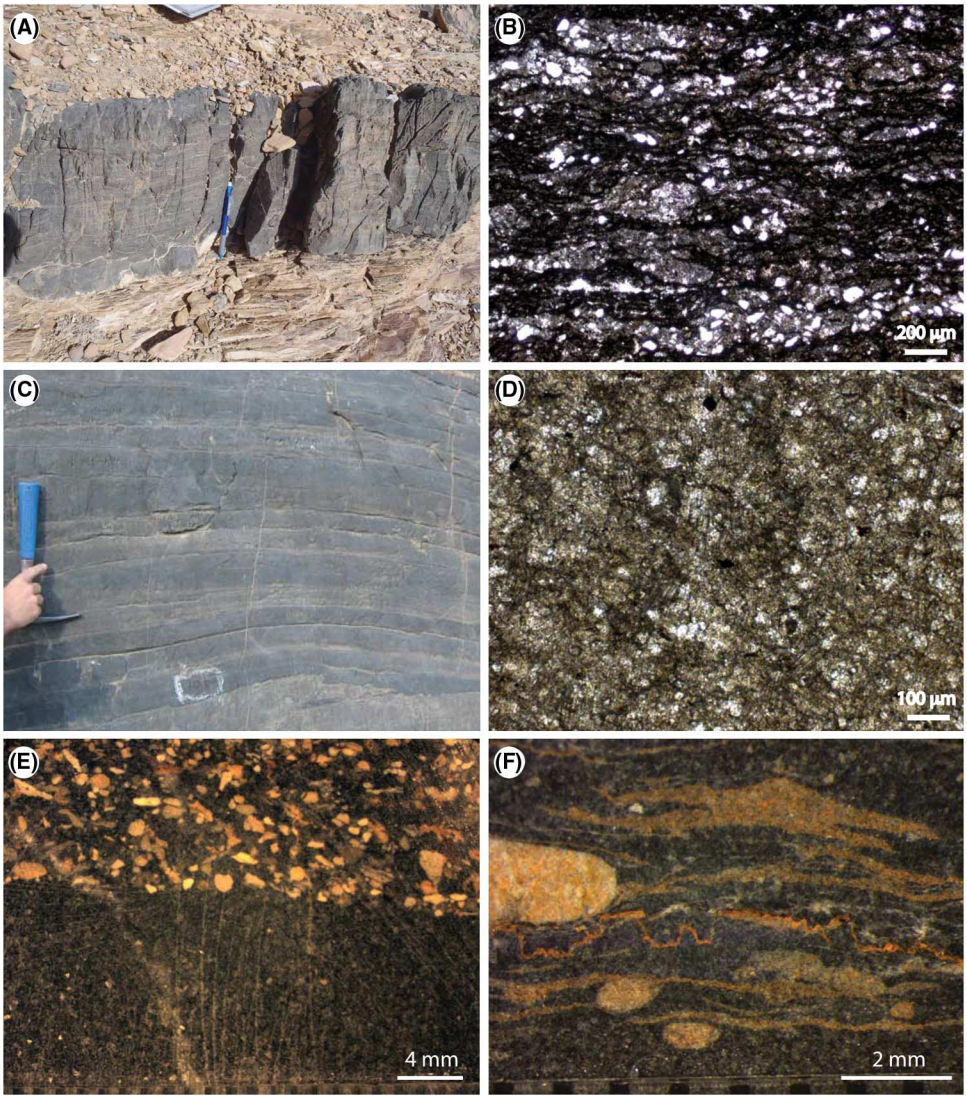

Figure 13. Transitional facies and carbonate dominated, Oman Mountains. (A) Lensoidal bed of crinkly laminite in outcrop surrounded by pink and yellow Masirah Bay siltstone, Wadi Sahtan; pencil is 15 cm (6 in.) long. (B) WM1 16A photomicrograph, crinkly laminite facies showing dark irregular micritic laminations binding quartz silt and very fine grained calcite sediment. (C) Graded intraclast grainstone beds from Wadi Hajir (hammer is 30 cm [12 in.] tall). (D) Photomicrograph of recrystallized peloidal wackestone/packstone. (E) WH1 intraclast grainstone slab in reflected light showing a bed boundary with recrystallized calcite matrix and micritic dolomite clasts of a graded bed scouring a finer grainstone below, scale in millimeters. (F) WM1 pebble conglomerate showing well-rounded dolomite pebbles draped with irregular laminae. Stylolite crosscuts image. Scale is in millimeters.

Carbonate-Dominated Facies Tract

The main body of the Khufai Formation in the Oman Mountains is a thin-bedded black limestone consisting primarily of graded intraclast wackestone and packstone, with minor accumulations of pebble grainstone to conglomerate, lime mudstone, graded grainstone, and slumped quartz sandstone. Although the prevailing grain size varies between these facies, common sedimentary structures across beds of different mean grain size indicate similar depositional processes.

Graded Intraclast Wackestone and Packstone

Graded intraclast wackestone and packstone are the predominant facies of the carbonate-dominated facies tract. Bedding is thin, and beds are grouped into meter-scale units of similar grain size, character, and thickness (Figure 13C). Pervasive neomorphic recrystallization of calcite precludes accurate determination of grain sizes except where coarse grains appear (Figure 13D). Angular dolomudstone clasts are normally graded with matrix material (Figure 13E). Scouring is common at bed bases, and soft sediment deformation such as ball and pillow and flame structures commonly accompany the coarsest beds. This facies is interpreted to represent deep-water turbidity currents originating along the steeper parts of the ramp at times of significant carbonate productivity (Schlager et al., 1994). Variability in bed thickness and grain size may correspond both to proximity to the main channelized flow path in a

submarine-fan complex, in addition to retrogradation and progradation patterns associated with highstand versus lowstand deposition (Betzler et al., 1999).

Coarse-Graded Grainstones

The coarsest beds in this system are graded peloid to ooid grainstones to pebble conglomerates. These grainstones are similar in bedding character to the packstone facies but lack mud matrix and are composed of well-rounded dolomudstone clasts and degraded ooids. Coarser beds contain larger rounded intraclasts and commonly have draping irregular muddy laminations (Figure 13F). Coarse beds increase in abundance approaching the sequence boundary, at higher order cycle tops, and approaching the MFI. Ghost rims of ooids are sometimes visible. Crosscutting diagenetic fabrics include an orbicular fabric and thick calcite spar veins. Increased grain size and character of clasts in this facies suggests transport from shallower on the ramp compared to the wackestone facies (Betzler et al., 1999). Lack of significant mudstone accumulation and well-developed draping irregular laminations suggest sediment bypass.

Lime Mudstone

Massive mudstone beds occur rarely and only as a significant component at Wadi Mistal. These mudstones are light gray and homogeneous, occurring above wackestone beds and deformed by subsequent wackestone deposition. The deformation creates either fluid escape structures and contorted bedding or nodular bedding. The occurrence of mudstone in one of the thinnest, presumably more distal sections suggests formation through settling of suspended fines away from the main turbidite fan network.

Slumped Quartz Sandstone

The uppermost beds of coarse-graded grainstone progressively incorporate quartz sand. Beds of pure quartz sandstone with carbonate intraclasts occur in some sections and particularly Wadi Bani Awf. Zones of extensive soft sediment deformation and recumbent folding are associated with the stratigraphically lowest, thick sandstone beds. Wave-generated sedimentary structures are absent. Sandstone beds are interpreted to be chronostratigraphically equivalent with those in the upper Khufai and Mukhaibah domes, but are indicative of a deeper depositional environment. Because this transition to siliciclastic facies occurs at the Khufai-Shuram boundary, we interpret these facies as a switch from transported carbonate sediments to reactivation of a source of siliciclastic sediment during flooding after the already demonstrated platformwide lowstand.

SEQUENCE STRATIGRAPHY

A sequence-stratigraphic model of the Khufai Formation was constructed based on the correlation of parasequences and parasequence sets and mapping of key stratigraphic surfaces. There are 133–207 parasequences in each complete Khufai section in the Huqf outcrop area that combine into 34–45 PS1, 16 PS2, and 1.5 depositional sequences. Three formation-scale sequence-stratigraphic surfaces are observed, including an MFI low in the formation, a type-2 sequence boundary (SB) in peritidal to supratidal deposits of the upper formation, and a transgressive surface (TS) representing the onset of Shuram Formation siltstone deposition. The MFI is very subtle in outcrop as the facies of this interval are thick bedded and largely homogeneous. The SB is mostly visible in the Khufai and Buah domes where amalgamated tepee breccias indicate extremely low accommodation. Parasequence stacking shows an increase in parasequence thickness approaching the MFI and a systematic decrease approaching the sequence boundary. The upper transgressive boundary coincides with the lithostratigraphic formation boundary and is easily identified where exposed.

Parasequences

Representative stratigraphic logs from the Mukhaibah, Khufai, and Buah domes at three different stratigraphic intervals through the HST are shown in Figure 14A. These sections illustrate trends in parasequence composition during ramp progradation and may include either one parasequence or a small-scale parasequence set. The composition of each parasequence will be discussed in ascending stratigraphic order.

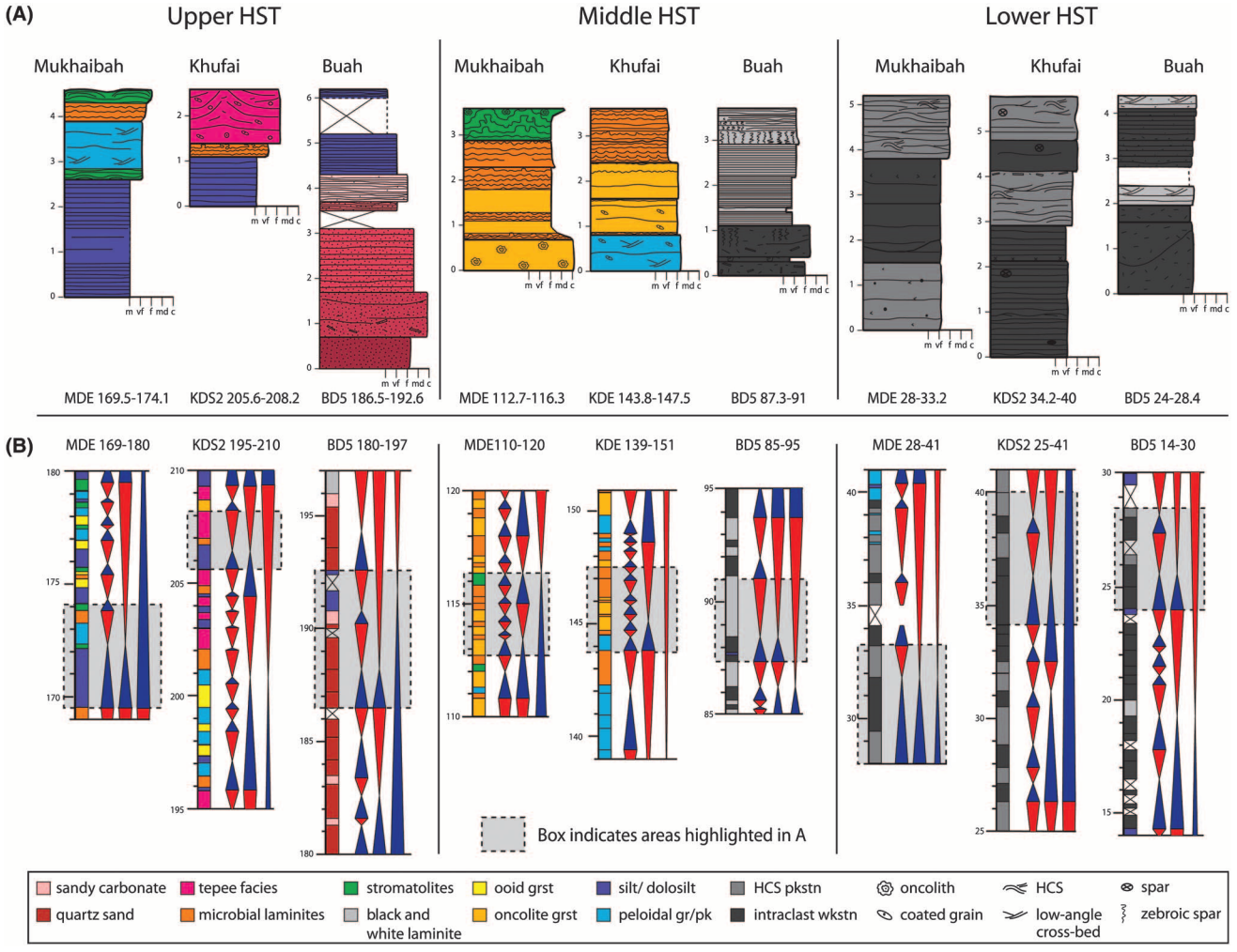

Figure 14. (A) Example stratigraphic sections from early, middle, and late highstand systems tracts (HST) illustrating parasequence to parasequence set-scale facies variability. B. Facies bars and transgressive-regressive triangles for intervals including sections from (A) (gray-shaded box). Triangle bars are arranged from left to right, parasequence, parasequence set, and composite parasequence set scales. Scales are in meters.

The lower HST deposits show the most homogeneous facies distributions. Parasequences are defined by subtle alteration in the influence of wave reworking on sedimentation patterns. The three domes show very similar facies distributions at this stratigraphic level, marked by interbedded intraclast wackestone and packstones and hummocky cross-stratified packstone facies (Figure 14A). At the Buah dome, the intraclast wackestones have larger clasts and the cross-bedding is tabular instead of hummocky.

In the middle HST, parasequence development is more prominent and involves a larger range of facies than lower in the formation. The largest difference compared to the lower HST is the appearance of coated grainstone and microbially dominated facies such as irregular laminite and oncolite grainstone. The Mukhaibah and Khufai domes show similar parasequence composition of oncolite grainstone-microbialite cycles. Each cycle base is defined by deposition of an oncolite or peloidal grainstone bed, followed by thin beds of alternating fine peloidal grainstone and irregular laminite, capped by a thick sequence of irregular or tufted laminite and/or stromatolite (Figure 14A). Grainstone-microbialite cycles frequently have an erosional base and desiccation features in the upper part of the cycle. This pattern is suggestive of a shallowing-upward

package culminating in very shallow water depths with intermittent exposure. Silicification of microbial facies enhances the appearance of cyclicity in this section. The middle HST facies patterns at the Buah dome instead show interbedded coarsely graded intraclast packstone beds capped with black and tan laminite. The black and tan laminite facies is interpreted to have formed in the middle ramp with storm-wave activity; the intraclast packstone represents an even deeper, outer-ramp setting. These cycles record shallowing, although at relatively greater water depths compared to the Khufai and Mukhaibah domes.

Parasequences of the upper highstand are diverse and vary considerably in both facies and thicknesses between outcrop areas (Figure 14A). At the Mukhaibah dome deposition of coated grainstone-microbialite cycles also incorporate lagoonal mudstones and siltstones at parasequence bases, in addition to more complex stromatolite morphologies. Relatively high-energy conditions are recorded at parasequence tops by an abundance of cross-bedding, especially climbing wave ripples. The upper HST of the Khufai dome is dominated by tepee-capped cycles. Lagoonal fines and fenestral mudstone are overlain by coated grainstone and/or microbialite as at the Mukhaibah dome; however, instead of stromatolite buildups, these cycles are capped by large tepee structures and associated breccias. The upper surfaces of tepees commonly are truncated, indicating further subaerial exposure after tepee formation. Where relief was preserved, lenses of sediment fill tepee polygons. Tepee-capped parasequences are thinner than those in the Mukhaibah dome (Figure 14A) likely because of sustained nondeposition and exposure events. Upper HST cycles at the Buah dome again differ from the southern Huqf and feature cyclic alternations of calcarenites to quartzarenites with interbedded black and tan laminite or siltstone facies (Figure 14A). Parasequences begin with relatively pure, thickly bedded, quartz sandstone with carbonate intraclasts and grade upward to more thinly bedded, carbonate-rich grainstone-sandstone mixtures. They are capped with silty carbonate beds and/or black and tan laminite. The presence of carbonate intraclasts in the basal sandstones is consistent with erosion of underlying carbonates during deposition and demarcates the cycle base.

Parasequence Stacking Patterns

Parasequence stacking patterns are documented by plotting transgressive-regressive cycles using blue and red triangles, respectively (Figures 14B, 15, 16). Figure 14B illustrates the parasequence, parasequence set (PS1), and composite parasequence set (PS2) for each of the representative parasequences discussed above. This analysis allows for comparison of scales of cyclicity both in a given area through the HST deposits, as well as between domes. General trends include a decrease in parasequence thickness approaching sequence boundaries. Comparison between domes reveals that the Khufai dome has the greatest number of preserved cycles, whereas the Buah dome has fewer, thicker cycles.

Extending this analysis to the whole formation shows longer term trends (Figures 15, 16). Figure 15 presents a PS1-scale correlation between stratigraphic sections in the Huqf area and includes PS2 and sequence-scale transgressive-regressive cycles. An increase in accommodation up to the MFI in the lower Khufai Formation occurs, generally decreasing accommodation up to the main sequence boundary and increasing accommodation through the Khufai-Shuram transition. A significant PS2-order sequence boundary occurs four cycles below the main SB. Although the formation-scale sequence boundary was chosen based on the clear accommodation minimum and evidence for subaerial exposure in the Khufai dome, this lower boundary corresponds to an evident facies change including the introduction of lagoonal facies and increased stromatolite growth in both the Khufai and Mukhaibah domes, both of which continue to intensify after the main SB.

This analysis is repeated for the Khufai Formation in the Oman Mountains and is illustrated in Figure 16. Despite the 400 km (240 mi) separating the Huqf and Oman Mountains outcrops, the MFI occurs in the transitional Masirah Bay-Khufai member of all sections, followed by a PS2-scale SB near the onset of carbonate deposition. A whole PS2 cycle occurs within the carbonate-dominated facies tract up to the main SB but varies considerably in thickness ranging from 60 to 85 m (197 to 279 ft) in Wadi Sahtan (WS1) and Wadi Hajir (WH1) compared to 10 and 15 m (33 and 49 ft) in Al Aqor

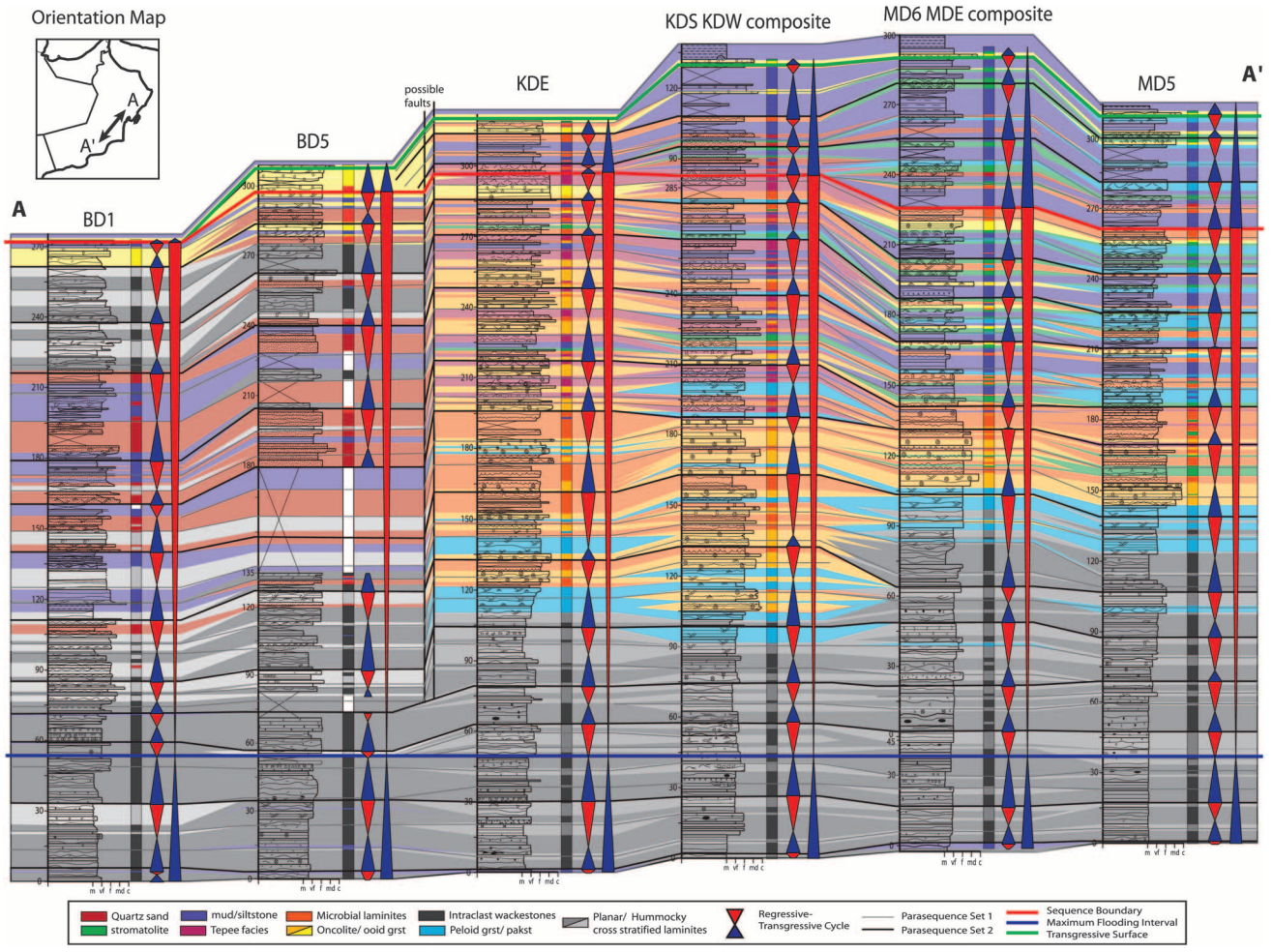

Figure 15. Detailed sequence-stratigraphic correlation of stratigraphic sections from the Huqf area highlighting transgressive-regressive cycles and facies variability. Colored columns show facies components of each section; colored wedges correlate coarse facies breakdown between sections. Transgressive-regressive cycles are shown at the composite parasequence set and sequence scale. Parasequence-set boundaries are shown in thin black lines, sequence-stratigraphic surfaces are shown in thick colored lines; see key. No horizontal scale.

(AQ1) and Wadi Mistal (WM1), respectively. This discrepancy accounts for a large part of the differences in thickness between the sections and for the very thin bedding and mud-dominated deposition of this part of AQ1 and WM1, respectively. An abrupt transition back to wackestone facies marks the sequence boundary, followed by the transgression into the Shuram Formation.

DISCUSSION

In this section, we discuss the environmental context of Khufai Formation deposition, including depositional environment, ramp geometry, eustatic trends, and the source of siliciclastic material. In addition, we will explore the function of syndepositional faulting in producing the unusual facies and stratigraphic geometries present at the Buah dome. Finally, we will address the potential of the Khufai Formation for future hydrocarbon exploration and development.

Depositional Environments

The Khufai Formation was deposited as a low-angle ramp complex on an arid, siliciclastic sediment-starved margin. The Khufai Formation thins significantly in

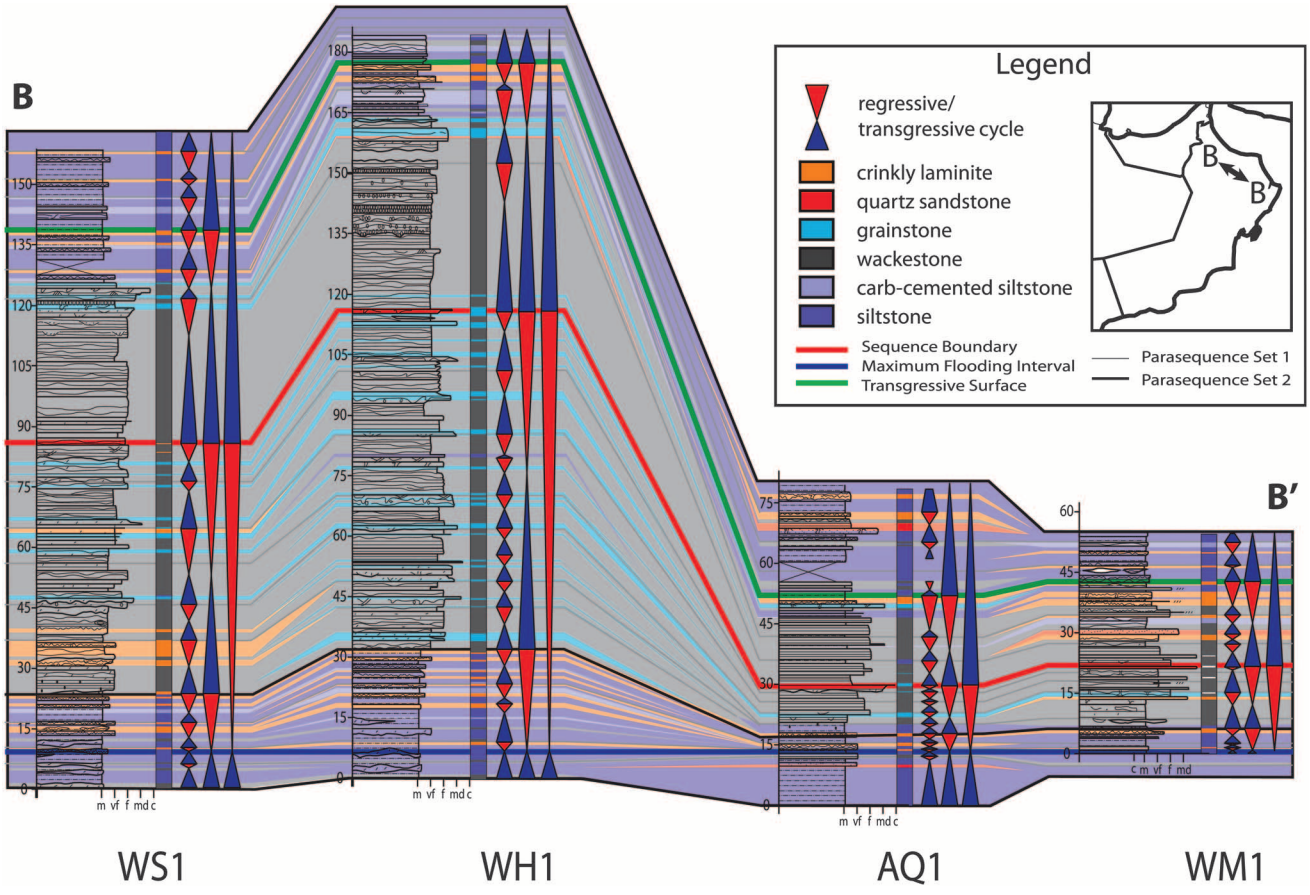

Figure 16. Sequence-stratigraphic correlation of stratigraphic sections from the Oman Mountains highlighting transgressive-regressive cycles and facies distributions. Colored bars show facies distributions; colored wedges correlate major facies patterns between sections. Sequence-scale transgressive-regressive cycles are shown at the parasequence set, composite parasequence set, and sequence scale. Stratigraphic surfaces are given in the key. No horizontal scale.

the Oman Mountains, matching trends in water depth for the underlying Masirah Bay Formation (Allen and Leather, 2006) which suggest deeper water sedimentation and condensation of the section. The transition between shallow- and deep-water sections is not exposed, preventing detailed assessment of the shelf-to-basin transition. Although the Khufai Formation has a layer-cake appearance, strong lateral facies variability is present. The distribution of the most variable facies is directly dependent on accommodation and the supply of siliciclastic sediment. Where siliciclastics were a minor component, transitions between peritidal grainstone and microbial buildup facies dominated shallow-water sedimentation patterns. Where siliciclastic sedimentation was high, such as at the Buah dome, sands were incorporated into peritidal grainstone intervals, and microbial components are absent. Varying levels of restriction in the inner lagoon environment created the extensive tepee belts present in the Khufai dome compared to the stromatolite-dominated Mukhaibah dome.

Ramp Geometry

The trends observed in parasequence stacking patterns can be used to extrapolate the geometry of the whole ramp complex for important times in its evolution. A dip-oriented cross section diagram (Figure 17) indicates the ramp is subdivided into five time intervals (T1–T4) that illustrate its evolution. The solid and dashed boxes indicate the approximate extent of the observable outcrop area in the Huqf and Oman Mountains, respectively.

The cross section begins at the sequence boundary in the Masirah Bay Formation (Allen and Leather, 2006). The T1 interval illustrates the TST

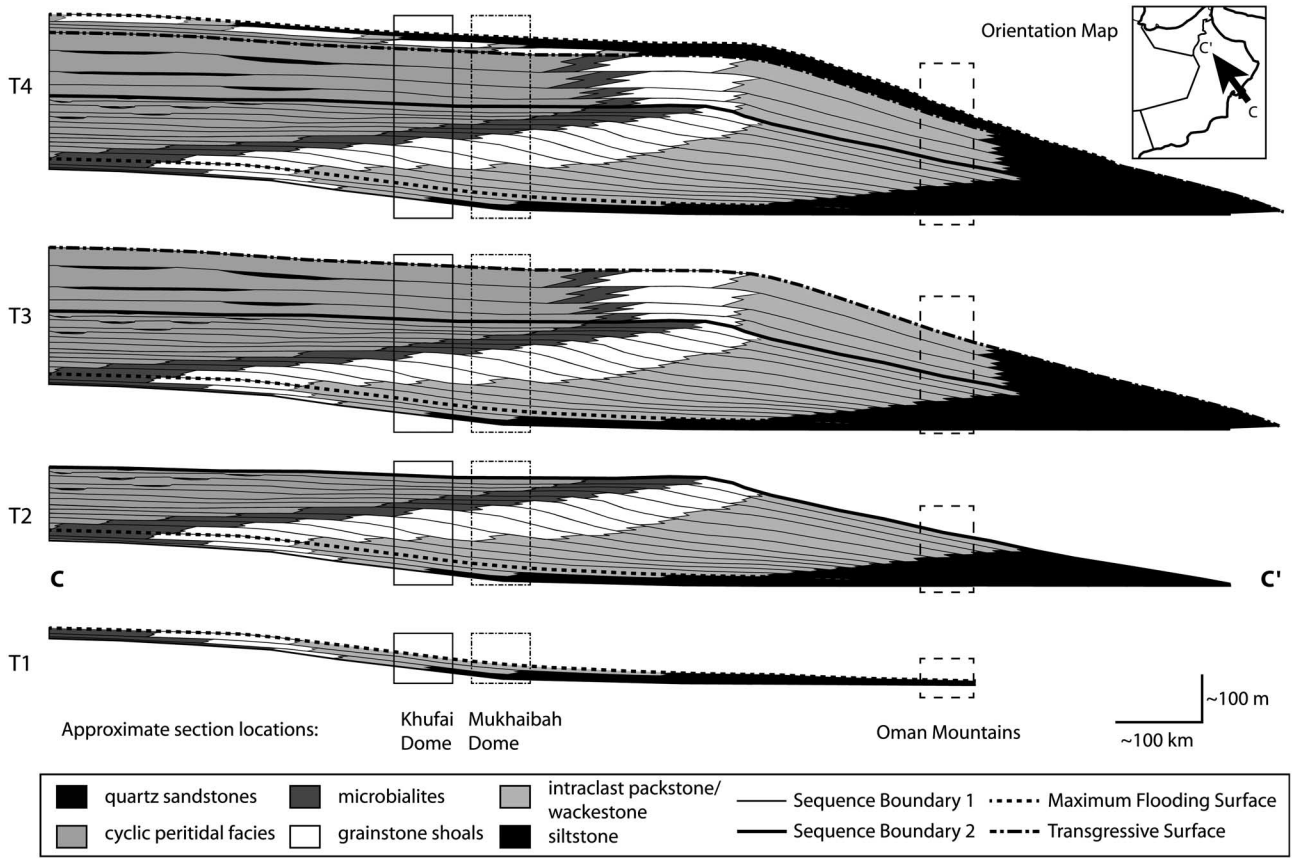

Figure 17. Schematic depositional profiles of the Khufai though four major time steps. Boxes show approximate zones of the Khufai dome, Mukhaibah dome, and Oman Mountain outcrop exposures. T1: SB in the Masirah Bay formation up through the maximum flooding surface in the lower Khufai Formation. T2: MFS up to SB2. T3: SB2 up to the transgressive surface. T4: Flooding into the Shuram Formation. Map inset shows approximate primary ramp orientation.

between this sequence boundary and the MFI in the lower Khufai Formation, showing the simultaneous flooding and decrease in siliciclastic supply. Increased carbonate production and export to downdip parts of the ramp ensued, resulting in the intraclast wackestone and packstone facies.

The T2 interval illustrates ramp evolution from the maximum flooding surface (MFS) up to the main SB in the Khufai Formation. This HST includes most of the Khufai Formation. The shoal complex is inferred to have had very low relief at the beginning, but its relief increased slightly through time. Increased restriction of the ramp as a whole is attributed to decreased circulation from the shoal complex barrier and decreased accommodation within the inner lagoons. Late highstand deposition occurs after the shoal complex prograded beyond the outcrop areas and includes restricted microbial flats and cyclic peritidal deposits. Increasing contributions of restricted lagoonal facies suggest continued expansion of the inner ramp. Parasequence thickness decreases throughout this interval and approaches a minimum during the late highstand.

The T3 interval shows increasing parasequence thickness up to a TS after the main SB. Lagoonal facies are thick and extensive in this interval, and large domal stromatolites appear at the Khufai and Mukhaibah domes. The uppermost parasequence capping stromatolites at the Mukhaibah dome become highly elongate, consistent with strong wave currents (cf. Grotzinger, 1986). These changes are likely tied to the building of the ramp crest and increased accommodation within the inner ramp. Sediment grain types change significantly as well with the replacement of oncoids with ooids as the dominant coated grain type along with the influx of siliciclastic sand. Although

oolites are rare in most of the Khufai Formation, their few occurrences are similar to the TS marker bed and foreshadow the transgression.

The T4 interval illustrates the dramatic transgressive surface of the upper Khufai Formation transitioning into the lowermost Shuram Formation. This surface is marked by a very coarse intraclast oolite and associated meter-scale muddy stromatolite bioherms before flooding into hummocky cross-stratified–bearing dolomudstone and red Shuram siltstone. The MFS within the lower Shuram Formation is generally not exposed but, where visible, contains dark-red siltstone.

Eustatic Trends

Khufai parasequence stacking patterns vary from high-frequency, low-amplitude trends approaching the sequence boundary to low-frequency, moderate-amplitude trends afterward. These changes can be interpreted to reflect eustatic variability in greenhouse versus icehouse conditions (Read, 1995; Elrick, 1996; Pope and Read, 1998) or, alternatively, changes in sediment supply and export (Burgess, 2001). Deconvolving these trends can be challenging, but detailed analysis of the facies variability can be helpful. A net decrease in parasequence thickness through the main HST is evident, along with a change in the visually dominant scale of cyclicity to PS from PS1 (Figure 15). The facies variability within each parasequence in this interval generally only includes two or three facies coincident with a relatively small range in water depth (1–3 m [3.3–10 ft]). This changes above the sequence boundary where the PS scale of cyclicity becomes difficult to observe, and instead, PS1 or PS2 scales of variability dominate outcrop and facies patterns, incorporating much larger numbers of facies and ranges of water depth (Figure 4A, 15); similar trends occur in the Oman Mountains (Figure 16).

The environmental context of the terminal Khufai Formation has significant implications for the Shuram carbon isotopic excursion, specifically whether the end of carbonate deposition relates to flooding by a eustatic mechanism or a more exotic geochemical mechanism (Le Guerroue and Cozzi, 2010; Grotzinger et al., 2011). Although this study does not address the potential geochemical causes specifically, data presented here indicate that the Khufai-Shuram boundary is marked by strong transgression with evidence for continued carbonate deposition, similar to what is observed in other globally distributed strata that preserve the Shuram excursion (Grotzinger et al., 2011). This suggests a eustatic control on flooding, consistent with the return of open-marine facies and parasequence stacking patterns indicative of a major increase in accommodation. Strata deposited just prior to the transgression reflect a gradual change to less restricted conditions and do not contain evidence for a significant hiatus. Furthermore, continuation of carbonate deposition (oolites) and cementation into the Shuram Formation is inconsistent with an environmental collapse of the carbonate factory and instead points to increased siliciclastic sediment supply as the driver of lithological change. Overall, we suggest that the transition from the Khufai Formation to the Shuram was a change in the balance between siliciclastic and carbonate deposition reflective of a strong transgressive event.

Clastic Input

Quartz sand occurs in three zones within the Khufai stratigraphy: the upper peritidal facies of the Khufai and Mukhaibah domes, throughout the calcarenites to quartzarenites of the Buah dome, and in deformed upper beds of the Oman Mountains. The former two instances were interpreted as tidal channels cutting through the middle ramp of the Huqf region (McCarron, 1999). In contrast, the Huqf sands were interpreted as inner-ramp tidal channels that cut through carbonate tidal-flat deposits (Gorin et al., 1982). A beach origin for the thin sandstones in the Khufai and Mukhaibah domes was hypothesized, and the grainstone and sandstone at the Buah dome were not differentiated in Wright et al. (1990). An eastward source of the sand was interpreted and fed from an onshore zone of deflation where sand was produced and subsequently blown into and reworked in the marine realm (Gorin et al., 1982; McCarron, 1999).

We suggest that termination of distal siliciclastic sedimentation at the beginning of Khufai Formation

deposition resulted from drowning of the clastic source during marine transgression. It is implied that a source area for siliciclastics was exposed updip of the preserved outcrop areas during marine regression. The arid setting is consistent with active eolian sand dune formation, although all of the sand bodies in the Khufai Formation show evidence of both wave reworking and combination with marine carbonate sediments (ooids, coated sand grains). Phelps et al. (2008) suggested that the sands were deposited in the marine realm but were likely introduced by eolian and local fluvial processes and reworked during parasequence-scale flooding events as evidenced in the Permian San Andres Formation. The models presented previously describing the small deposits of sand in the southern Huqf as tidal channels are consistent with our observations (Gorin et al., 1982). The nonwave-reworked, slumped sands in the Oman Mountains were likely emplaced as mass flows downslope in a deeper environment.

The large accumulations of mixed quartz sand and carbonate grains at the Buah dome require further explanation. Modern arid carbonate-producing environments in the Persian Gulf provide significant insight into the source of siliciclastics in the Khufai ramp. The Holocene leeward coast of the Qatar Peninsula has migrating eolian sand dunes that transport sand directly into marine carbonate-producing areas (Shinn, 1973b). These sands are incorporated into carbonate deposits as meter-scale beds of wave-reworked fine to medium sandstone. The description of these deposits is consistent with the sedimentological and depositional patterns observed at the Buah dome. The scale of facies heterogeneity in the Khufai Formation mirrors variation in the modern-day Arabian coast and reflects complex shoreline geometries, with strong lateral gradients in sediment supply (Shinn, 1973a, b).

Previous studies of mixed clastic-carbonate systems have demonstrated the stratigraphic controls on sand-body accumulation (Kerans et al., 1994; McNeill et al., 2004; Barnaby and Ward, 2007; Phelps et al., 2008). In the Permian Basin of west Texas, bypass of eolian sand into downslope environments is well documented (Phelps et al., 2008). Sequence boundaries sit directly below packages of siliciclastics, suggesting that Khufai sands also may have accumulated during increases in accommodation. The potential source of this accommodation will be discussed in the following section.

Synsedimentary Faulting

Although the Buah dome is in close proximity to other Huqf exposures, its depositional patterns differ significantly from the simple ramp model and may suggest the influence of syndepositional faulting. This hypothesis is based on abrupt lateral facies changes, very coarse, deformed, conglomeratic wackestones in the late HST, and incorporation of larger amounts of siliciclastic material. Figure 15 illustrates the abrupt lateral facies differences between Buah dome 5 (BD5) and Khufai dome east (KDE), which are separated by only 13.3 km (8.3 mi) and lie along a depositional strike-parallel trend. For instance, throughout the Huqf region, facies and parasequence stacking patterns at all domes indicate shallowing to an accommodation minimum in the top 60–80 m (197–242 ft) of section; however, facies and stacking patterns after this point at the Buah dome diverge and contain thick packages of outer- to middle-ramp deposits. This contrasts with the much greater lateral uniformity of facies between MD5 and KDE that spans a distance of approximately 35 km (22 mi) (Figure 15).

Additional support for synsedimentary faulting comes from the interpretation of intraclast wackestone facies and soft sediment deformation features at the Buah dome. The intraclast wackestone and packstone facies at the Buah dome frequently contains uncommonly large clasts (centimeter to decimeter scale). Although this difference is relatively minor in the base of the section, it increases near the top of the formation to include coarse pebble to cobble-size clasts and breccia layers. These beds are associated with large-scale slumping, contorted beds, and fluid escape structures and resemble seismites produced in carbonates or mixed sedimentary systems (Pope et al., 1997; Onasch and Kahle, 2002). Although similar features can be produced by loading, storm or tidal reworking, or gravity-driven slumping, the lateral continuity, size, and stratigraphic context of these features suggests faulting (Greb and Denver, 2002; Wheeler, 2002). The

presence of early cemented shallow-water carbonates in the intraclast breccias at the Buah dome may indicate a fault-induced depth gradient.

Finally, the presence of thick siliciclastic deposits at the Buah dome also is consistent with synsedimentary faulting. Regional correlation across the Huqf area suggests that sand bodies at the Buah dome accumulated as other parts of the platform experienced extremely low accommodation and sediment bypassing (Figure 15). The parasequence thickness patterns indicate that this does not simply represent a change in position relative to the regional shoreline, but instead increased accommodation and accumulation of eolian sands that would have otherwise bypassed at times of sea level lowstand.

These lines of evidence for synsedimentary faulting are largely circumstantial because little is known about the nature of the faults themselves. No small-scale growth faults are directly observed in outcrop that might confirm this hypothesis. However, significant thickness and facies variability were noted in the Masirah Bay and Buah Formations (Cozzi and Grotzinger, 2004; Allen and Leather, 2006). These observations all are consistent with the possibility of local tectonic activity during Khufai Formation deposition. It appears that a long-lived structure that bisects the Buah dome—the Maradi fault—may have expressed itself during Nafun deposition and influenced sedimentation patterns all through the Phanerozoic history of this part of Oman (Hanna and Nolan, 1989).

Implications for Hydrocarbon Exploration

The Khufai Formation contains facies with both depositional and diagenetic potential as hydrocarbon reservoirs. Dolomitized carbonates worldwide have proven to be very successful reservoirs (Alsharhan and Nairn, 1997; Ahr, 2008). Although most are younger than the Khufai Formation, proven plays in the overlying Ara Group suggest excellent preservation and seal quality (Al-Siyabi, 2005).

Although very low in total organic carbon (generally <0.05%), the lower Khufai Formation is petroliferous, particularly in zones of extensive recrystallization, which may serve to concentrate mobile hydrocarbon. The facies in the Oman Mountains are H_2S rich instead of petroliferous, but their black color speaks to a history rich in organic carbon. Additional source rock potential comes from the underlying shales of the Masirah Bay Formation that are organic rich (Terken et al., 2001; Grosjean et al., 2009).

The reservoir potential of the Khufai Formation is considerable, but diagenetic factors such as subsurface cementation history will require more exploration. Coarse oncolite grainstone facies of the middle to late HST are likely reservoir candidates. However, in outcrop, significant porosity-occluding silicification has occurred; it is not known to what extent silicification has impacted the subsurface. In contrast, recrystallization and dolomitization processes in the lower Khufai Formation were extensive and acted to create pockets of extremely coarsely crystalline, porous material. The degree of interconnectivity of these pockets will be very important for exploration. Perhaps the most promising potential reservoir facies of the Khufai Formation are the quartz sandstones within the Buah dome. These sands are poorly cemented in outcrop and are capped with either tight intraclast wackestone facies or siltstone. The position of these deposits on the margin of an active tectonic system (as at the Buah dome) suggests the possibility of more widespread sand incorporation in other paleolows. Although the lateral extent of this facies in the subsurface is unknown, because of structural and environmental complexity, mapping with traditional well techniques may be very informative.

CONCLUSIONS

- The Khufai Formation records continuous deposition of a carbonate ramp during the Ediacaran Period. It contains three major sequence-stratigraphic surfaces that define one and one-half depositional sequences. Most of the Khufai Formation comprises an HST and records progradation of the ramp, capturing facies ranging from outer-ramp to supratidal depositional environments. Distal-ramp depositional environments are recorded in the Oman Mountains. Parasequence-stacking patterns reveal a transition from high-frequency,

low-amplitude to low-frequency, moderate-amplitude sea level oscillation at the sequence boundary.

- This carbonate platform displays considerable facies variability and depositional complexity introduced from siliciclastic sediment supply and potentially syndepositional faulting. Siliciclastic input is most prevalent in the northern Huqf where large quantities of quartz sandstone are incorporated with and replace carbonate facies. Discrepancies between this area and the other platform locations along with seismite facies suggest the potential for previously undocumented tectonism concurrent with deposition.
- Potential for hydrocarbon exploration and development exists in the Khufai Formation with potential source (basal mudstone), reservoir (oncolite grainstone, quartz sandstone, diagenetic fabrics), and seal facies (basal mudstones, Shuram Formation siltstones) being identified. However, further investigation of the subsurface cementation history and the connectivity of high-porosity facies groups will be required.
- The boundary between the Khufai and Shuram Formations is not a major unconformity and is instead marked by rapid transgression and a return to deeper water, siliciclastic-dominated deposition. Accordingly, this boundary cannot account for the missing time between dated intervals of the Huqf Supergroup as suggested by other authors. Although a sequence boundary does occur within the upper Khufai Formation, it is well below the Khufai-Shuram lithostratigraphic boundary and the onset of the Shuram isotopic excursion.

REFERENCES CITED

Ahr, W. M., 2008, Geology of carbonate reservoirs: Identification, description, and characterization of hydrocarbon reservoirs in carbonate rocks: Wiley-Interscience, 296 p.

Allen, P. A., 2007, The Huqf Supergroup of Oman: Basin development and context for Neoproterozoic glaciation: Earth-Science Reviews, v. 84, p. 139–185, doi: 10.1016/j.earscirev.2007.06.005.

Allen, P. A., and J. Leather, 2006, Post-Marinoan marine siliciclastic sedimentation: The Masirah Bay Formation, Neoproterozoic Huqf Supergroup of Oman: Precambrian Research, v. 144, no. 3–4, p. 167–198, doi: 10.1016/j.precamres.2005.10.006.

Allen, P. A., J. Leather, M. Brasier, R. Rieu, M. McCarron, E. Le Guerroue, S. Bowring, J. Grotzinger, J. Etienne, and A. Cozzi, 2011, The Abu Mahara Group (Ghubrah and Fiq Formations), Jabal Akhdar, Oman: Geological Society (London) Memoir 36, p. 251–262.

Alsharhan, A. S., and A. E. M. Nairn, 1997, Sedimentary basins and petroleum geology of the Middle East: Amsterdam, Elsevier Science, 942 p.

Al-Siyabi, H. A., 2005, Exploration history of the Ara intrasalt carbonate stringers in the South Oman salt basin: GeoArabia, v. 10, no. 4, p. 39–54.

Assereto, R. L., and C. Kendall, 1977, Nature, origin and classification of peritidal tepee structures and related breccias: Sedimentology, v. 24, p. 153–210, doi: 10.1111/j.1365-3091.1977.tb00254.x.

Barnaby, R. J., and W. B. Ward, 2007, Outcrop analog for mixed siliciclastic-carbonate ramp reservoirs—Stratigraphic hierarchy, facies architecture, and geologic heterogeneity: Grayburg Formation, Permian Basin, U.S.A.: Journal of Sedimentary Research, v. 77, p. 34–58.

Betzler, C., J. Reijmer, K. Bernet, G. Eberli, and F. Anselmentti, 1999, Sedimentary patterns and geometries of the Bahamian outer carbonate ramp (Miocene–lower Pliocene, Great Bahama bank): Sedimentology, v. 46, p. 1127–1143, doi: 10.1046/j.1365-3091.1999.00268.x.

Bowring, S. A., J. P. Grotzinger, D. J. Condon, J. Ramezani, M. J. Newall, and P. A. Allen, 2007, Geochronologic constraints on the chronostratigraphic framework of the Neoproterozoic Huqf Supergroup, Sultanate of Oman: American Journal of Science, v. 307, no. 10, p. 1097–1145, doi: 10.2475/10.2007.01.

Brasier, M., G. McCarron, R. Tucker, J. Leather, P. Allen, and G. Shields, 2000, New U-Pb zircon dates for the Neoproterozoic Ghubrah glaciation and for the top of the Huqf Supergroup, Oman: Geology, v. 28, no. 2, p. 175–178, doi: 10.1130/0091-7613(2000)28<175:NUZDFT>2.0.CO;2.

Burchette, T., and V. Wright, 1992, Carbonate ramp depositional systems: Sedimentary Geology, v. 79, no. 3, p. 3–54.

Burgess, P. M., 2001, Modeling carbonate sequence development without relative sea-level oscillations: Geology, v. 29, no. 12, p. 1127–1130, doi: 10.1130/0091-7613(2001)029<1127:MCSDWR>2.0.CO;2.

Burns, S. J., and A. Matter, 1993, Carbon isotopic record of the latest Proterozoic from Oman: Eclogae Geologicae Helvetiae, v. 86, no. 2, p. 595–607.

Carto, S. L., and N. Eyles, 2011, The deep-marine glaciogenic Gaskiers Formation, Newfoundland, Canada: The geological record of Neoproterozoic glaciations: Geological Society (London) Memoirs, v. 36, no. 1, p. 467–473.

Cozzi, A., and J. Grotzinger, 2004, Evolution of a terminal Neoproterozoic carbonate ramp system (Buah Formation, Sultanate of Oman): Effects of basement paleotopography: Geological Society of America Bulletin, v. 116, no. 11–12, p. 1367–1384, doi: 10.1130/B25387.1.

Cozzi, A., P. A. Allen, and J. P. Grotzinger, 2004, Understanding carbonate ramp dynamics using $\delta^{13}C$ profiles: Examples

from the Neoproterozoic Buah Formation of Oman: Terra Nova, v. 16, no. 2, p. 62–67, doi: 10.1111/j.1365-3121.2004.00528.x.

Dibenedetto, S., and J. Grotzinger, 2005, Geomorphic evolution of a storm-dominated carbonate ramp (c. 549 Ma), Nama Group, Namibia: Geological Magazine, v. 142, no. 5, p. 583–604, doi: 10.1017/S0016756805000890.

Elrick, M., 1996, Sequence stratigraphy and platform evolution of Lower–Middle Devonian carbonates, eastern Great Basin: Geological Society of America Bulletin, v. 108, no. 4, p. 392–416, doi: 10.1130/0016-7606(1996)108<0392:SSAPEO>2.3.CO;2.

Elrick, M., and J. Read, 1991, Cyclic ramp-to-basin carbonate deposits, lower Mississippian, Wyoming and Montana: A combined field and computer modeling study: Journal of Sedimentary Research, v. 61, no. 7, p. 1194–1224.

Eyles, N., and C. H. Eyles, 2006, Glacially-influenced deep-marine sedimentation of the Late Precambrian Gaskiers Formation, Newfoundland, Canada: Sedimentology, v. 36, no. 4, p. 601–620, doi: 10.1111/j.1365-3091.1989.tb02088.x.

Fairchild, I., 1991, Origins of carbonate in Neoproterozoic stromatolites and the identification of modern analogs: Precambrian Research, v. 53, p. 281–299, doi: 10.1016/0301-9268(91)90076-M.

Fairchild, I., and P. Herrington, 1989, A tempestite-stromatolite-evaporite association (late Vendian, East Greenland): A shoreface-lagoon model: Precambrian Research, v. 43, p. 101–127, doi: 10.1016/0301-9268(89)90007-7.

Fike, D. A., and J. P. Grotzinger, 2008, A paired sulfate–pyrite $\delta^{34}S$ approach to understanding the evolution of the Ediacaran–Cambrian sulfur cycle: Geochimica et Cosmochimica Acta, v. 72, p. 2636–2648, doi: 10.1016/j.gca.2008.03.021.

Fike, D. A., J. P. Grotzinger, L. M. Pratt, and R. E. Summons, 2006, Oxidation of the Ediacaran Ocean: Nature, v. 444, no. 7120, p. 744–747, doi: 10.1038/nature05345.

Forbes, G., H. Jansen, and J. Schreurs, 2010, Lexicon of Oman subsurface stratigraphy: Manama, Bahrain: GeoArabia, Special Publication 5, p. 371.

Goldhammer, R. K., P. A. Dunn, and L. A. Hardie, 1990, Depositional styles, composite sea-level changes, cycle stacking patterns, and the hierarchy of stratigraphic forcing: Examples from Alpine Triassic platform carbonates: Geological Society of America Bulletin, v. 102, p. 535–562, doi: 10.1130/0016-7606(1990)102<0535:DCCSLC>2.3.CO;2.

Gorin, G., L. Racz, and M. Walter, 1982, Late Precambrian–Cambrian sediments of the Huqf Supergroup, Sultanate of Oman: AAPG Bulletin, v. 66, p. 2209–2627.

Greb, S. F., and G. R. J. Denver, 2002, Critical evaluation of possible seismites: Examples from the Carboniferous of the Appalachian basin, *in* F. R. Ettensohn, N. Rast, and C. E. Brett, eds., Ancient seismites: Geological Society of America Bulletin Special Papers, v. 359, p. 109–125.

Grosjean, E., G. D. Love, C. Stalvies, D. A. Fike, and R. E. Summons, 2009, Origin of petroleum in the Neoproterozoic–Cambrian South Oman salt basin: Organic Geochemistry, v. 40, no. 1, p. 87–110, doi: 10.1016/j.orggeochem.2008.09.011.

Grotzinger, J., 1986a, Evolution of early Proterozoic passive-margin carbonate platform, Rocknest Formation, Wopmay orogen, Northwest Territories, Canada: Journal of Sedimentary Petrology, v. 56, no. 6, p. 831–847.

Grotzinger, J. P., 1986b, Cyclicity and paleoenvironmental dynamics, Rocknest platform, northwest Canada: Geological Society of America Bulletin, v. 97, p. 1208–1231, doi: 10.1130/0016-7606(1986)97<1208:CAPDRP>2.0.CO;2.

Grotzinger, J. P., 1989, Facies evolution of Precambrian carbonate depositional systems: emergence of the modern platform archetype, *in* P. D. Crevello, J. L. Wilson, J. F. Sarg, and J. F. Read, eds., Controls on carbonate platform and basin development: SEPM Special Publication 44, p. 79–106.

Grotzinger, J., and J. Amthor, 2002, Facies and reservoir architecture of isolated microbial carbonate platforms, terminal Proterozoic–Early Cambrian Ara Group, South Oman salt basin: AAPG Annual Convention, Houston, Texas, v. 11, p. A67.

Grotzinger, J. P., and A. H. Knoll, 1999, Stromatolites in Precambrian carbonates: Evolutionary mileposts or environmental dipsticks?: Annual Review of Earth and Planetary Sciences, v. 27, p. 313–358, doi: 10.1146/annurev.earth.27.1.313.

Grotzinger, J., H. Al-Siyabi, R. Al-Hashimi, and A. Cozzi, 2002, New model for tectonic evolution of Neoproterozoic–Cambrian Huqf Supergroup basins, Oman: GeoArabia, v. 7, p. 241.

Grotzinger, J. P., D. A. Fike, and W. W. Fischer, 2011, Enigmatic origin of the largest-known carbon isotope excursion in Earth's history: Nature Geoscience, v. 4, no. 5, p. 285–292, doi: 10.1038/ngeo1138.

Halverson, G., 2005, Toward a Neoproterozoic composite carbon-isotope record: Geological Society of America Bulletin, v. 117, no. 9, p. 1181.

Hanna, S., and S. Nolan, 1989, The Maradi fault zone—Evidence of late Neogene tectonics in the Oman Mountains: Journal of the Geological Society, v. 146, p. 867–871, doi: 10.1144/gsjgs.146.5.0867.

Hebert, C. L., A. J. Kaufman, S. C. Penniston-Dorland, and A. J. Martin, 2010, Radiometric and stratigraphic constraints on terminal Ediacaran (post-Gaskiers) glaciation and metazoan evolution: Precambrian Research, v. 182, no. 4, p. 402–412, doi: 10.1016/j.precamres.2010.07.008.

Kendall, C., and J. Warren, 1987, A review of the origin and setting of tepees and their associated fabrics: Sedimentology, v. 34, p. 1007–1027, doi: 10.1111/j.1365-3091.1987.tb00590.x.

Kerans, C., and W. Fitchen, 1995, Sequence hierarchy and facies architecture of a carbonate-ramp system: San Andres Formation of Algerita escarpment and western Guadalupe Mountains, west Texas and New Mexico: Bureau of Economic Geology, Report of Investigations No. 235, p. 1–86.

Kerans, C., F. Lucia, and R. Senger, 1994, Integrated characterization of carbonate ramp reservoirs using Permian San Andres Formation outcrop analogs: AAPG Bulletin, v. 78, no. 2, p. 181–216.

Knoll, A. H., and K. Swett, 1990, Carbonate deposition during the late Proterozoic era: An example from Spitsbergen: American Journal of Science, v. 290-A, p. 104–132.

Koerschner, W., and J. Read, 1989, Field and modeling studies of Cambrian carbonate cycles, Virginia Appalachians: Journal of Sedimentary Petrology, v. 59, no. 5, p. 654–687.

Krinsley, D. H., P. F. Friend, and R. Klimentidis, 1976, Eolian transport textures on the surfaces of sand grains of Early Triassic age: Geological Society of America Bulletin, v. 87, p. 130–132, doi: 10.1130/0016-7606(1976)87<130:ETTOTS>2.0.CO;2.

Le Guerroue, E., and A. Cozzi, 2010, Veracity of Neoproterozoic negative C-isotope values: The termination of the Shuram negative excursion: Gondwana Research, v. 17, no. 4, p. 653–661, doi: 10.1016/j.gr.2009.11.002.

Le Guerroue, E., P. A. Allen, and A. Cozzi, 2006a, Chemostratigraphic and sedimentological framework of the largest negative carbon isotopic excursion in Earth history: The Neoproterozoic Shuram Formation (Nafun Group, Oman): Precambrian Research, v. 146, p. 68–92.

Le Guerroue, E., P. A. Allen, and A. Cozzi, 2006b, Parasequence development in the Ediacaran Shuram Formation (Nafun Group, Oman): High-resolution stratigraphic test for primary origin of negative carbon isotopic ratios: Basin Research, v. 18, no. 2, p. 205–219, doi: 10.1111/j.1365-2117.2006.00292.x.

Le Guerroue, E., P. A. Allen, A. Cozzi, J. L. Etienne, and M. Fanning, 2006c, 50 Myr recovery from the largest negative $\delta^{13}C$ excursion in the Ediacaran Ocean: Terra Nova, v. 18, no. 2, p. 147–153, doi: 10.1111/j.1365-3121.2006.00674.x.

Lehrmann, D., Y. Wan, J. Wei, Y. Yu, and J. Xiao, 2001, Lower Triassic peritidal cyclic limestone: An example of anachronistic carbonate facies from the Great Bank of Guizhou, Nanpanjiang Basin, Guizhou Province, South China: Palaeo, v. 173, p. 103–125, doi: 10.1016/S0031-0182(01)00302-9.

Markello, J., and J. F. Read, 1981, Carbonate ramp-to-deeper shale shelf transitions of an Upper Cambrian intrashelf basin, Nolichucky Formation, southwest Virginia Appalachians: Sedimentology, v. 28, p. 573–597, doi: 10.1111/j.1365-3091.1981.tb01702.x.

Mattes, B., and S. Conway Morris, 1990, Carbonate/evaporite deposition in the Late Precambrian–Early Cambrian Ara Formation of southern Oman, *in* A. H. F. Robertson, M. P. Searle, and A. C. Ries, eds., The geology and tectonics of the Oman region: Geological Society (London) Special Publication 49, p. 617–636.

McCarron, G. M., 1999, Sedimentology and stratigraphy of the Nafun Group: Huqf Supergroup, Oman, Doctor of Philosophy, Trinity College, Oxford University, 302 p.

McNeill, D. F., K. J. Cunningham, and L. A. Guertin, 2004, Depositional themes of mixed carbonate-siliciclastics in the south Florida Neogene: Application to ancient deposits, *in* G. M. Gramer, P. M. Harris, and G. P. Eberli, eds., Integration of outcrop and modern analogs to reservoir modeling: AAPG Memoir 80, p. 1–21.

Onasch, C. M., and C. F. Kahle, 2002, Seismically induced soft-sediment deformation in some Silurian carbonates, eastern U.S. midcontient, *in* F. R. Ettensohn, N. Rast, and C. E. Brett, eds., Ancient seismites: Geological Society of America Bulletin Special Papers, v. 359, p. 165–179.

Orpin, A., G. Brunskill, I. Zagorskis, and K. Woolfe, 2004, Patterns of mixed siliciclastic-carbonate sedimentation adjacent to a large dry-tropics river on the central Great Barrier Reef shelf, Australia: Australian Journal of Earth Sciences, v. 51, p. 665–683, doi: 10.1111/j.1400-0952.2004.01083.x.

Phelps, R. M., C. Kerans, S. Z. Scott, X. Janson, and J. A. Bellian, 2008, Three-dimensional modeling and sequence stratigraphy of a carbonate ramp-to-shelf transition, Permian Upper San Andres Formation: Sedimentology, v. 55, p. 1777–1813, doi: 10.1111/j.1365-3091.2008.00967.x.

Pope, M. C., and J. F. Read, 1998, Ordovician meter-scale cycles: Implications for climate and eustatic fluctuations in the central Appalachians during a global greenhouse, non-glacial to glacial transition: Palaeogeography, Palaeoclimatology, Palaeoecology, v. 138, p. 27–42, doi: 10.1016/S0031-0182(97)00130-2.

Pope, M. C., J. F. Read, R. Bambach, and H. J. Hofmann, 1997, Late Middle to Late Ordovician seismites of Kentucky, southwest Ohio and Virginia: Sedimentary recorders of earthquakes in the Appalachian Basin: Geological Society of America Bulletin, v. 109, no. 4, p. 489–503, doi: 10.1130/0016-7606(1997)109<0489:LMTLOS>2.3.CO;2.

Read, J., 1985, Carbonate platform facies models: AAPG Bulletin, v. 69, p. 1–21.

Read, J. F., 1995, Overview of carbonate platform sequences, cycle stratigraphy and reservoirs in greenhouse and ice house worlds, *in* J. F. Read, C. Kerans, L. J. Weber, J. F. Sarg, and F. M. Wright, eds., Milankovitch sea-level changes, cycles, and reservoirs on carbonate platforms in greenhouse and ice-house worlds: SEPM Short Course 35, p. 1–103.

Riding, R., 2000, Microbial carbonates: The geological record of calcified bacteria-algal mats and biofilms: Sedimentology, v. 47, no. 1, p. 179–214, doi: 10.1046/j.1365-3091.2000.00003.x.

Rieu, R., and P. A. Allen, 2008, Siliciclastic sedimentation in the interlude between two Neoproterozoic glaciations, Mirbat area, southern Oman: A missing link in the Huqf Supergroup?: GeoArabia, v. 13, no. 4, p. 45–72.

Sami, T. T., and N. P. James, 1994, Peritidal carbonate platform growth and cyclicity in an Early Proterozoic foreland basin, upper Pethei Group, northwest Canada: Journal of Sedimentary Research, v. B64, no. 2, p. 111–131.

Sami, T. T., and N. P. James, 1996, Synsedimentary cements as Paleoproterozoic platform building blocks, Pethei Group, northwestern Canada: Journal of Sedimentary Research, v. 66, no. 1, p. 209–222.

Schlager, W., J. Reijmer, and A. Droxler, 1994, Highstand shedding of carbonate platforms: Journal of Sedimentary Research, v. B64, no. 3, p. 270–281.

Shinn, E., 1973a, Carbonate coastal accretion in an area of longshore transport, NE Qatar, Persian Gulf, *in* B. H. Purser, ed., The Persian Gulf: New York, Heidelberg, Berlin, Springer-Verlag, p. 179–191.

Shinn, E., 1973b, Sedimentary accretion along the Leeward, SE Coast of Qatar Peninsula, Persian Gulf, *in* B. H. Purser, ed., The Persian Gulf: New York, Heidelberg, Berlin, Springer-Verlag, p. 199–209.

Shinn, E., R. Lloyd, and R. Ginsburg, 1969, Anatomy of a modern carbonate tidal-flat, Andros island, Bahamas: Journal of Sedimentary Research, v. 39, no. 3, p. 1202–1228.

Sumner, D., and W. Corcoran, 2001, Decimeter-thick encrustations of calcite and aragonite on the sea floor and implications for Neoarchean and Neoproterozoic ocean chemistry, *in* W. Altermann and P. L. Corcoran, eds., Precambrian sedimenatery environments: A modern approach to ancient depositional systems: International Association of Sedimentologists Special Publication 14, p. 107–120.

Terken, J. M. J., N. L. Frewin, and S. L. Indrelid, 2001, Petroleum systems of Oman: Charge timing and risks: AAPG Bulletin, v. 85, p. 1817–1845.

Tinker, S., 1998, Shelf to basin facies distributions and sequence stratigraphy of a steep-rimmed carbonate margin: Capitan depositional system, McKittrick Canyon, New Mexico and Texas: Journal of Sedimentary Research, v. 68, no. 6, p. 1146–1174, doi: 10.2110/jsr.68.1146.

Tucker, M., and V. Wright, 1990, Carbonate sedimentology: Blackwell Science, Oxford, United Kingdom, p. 482.

Wheeler, R., 2002, Distinguishing seismic from nonseismic soft-sediment structures: Criteria from seismic-hazard analysis, *in* F. R. Ettensohn, N. Rast, and C. E. Brett, eds., Ancient seismites: Geological Society of America Special Papers 359, 190 p.

Wilson, J., 1975, Carbonate facies in geologic history: London, Heidelberg, Berlin, Springer-Verlag, 471 p.

Wood, R., J. Grotzinger, and J. Dickson, 2002, Proterozoic modular biomineralized metazoan from the Nama Group, Namibia: Science, v. 296, no. 5577, p. 2383–2386, doi: 10.1126/science.1071599.

Wright, V., A. Ries, and S. Munn, 1990, Intraplatformal basin-fill deposits from the Infracambrian Huqf Group, east Central Oman, *in* A. Robertson, M. Searle, and A. Ries, eds., The geology and tectonics of the Oman region: Geological Society (London), p. 1–16.